

**POLITECNICO**  
**MILANO 1863**

Master of Science in Space Engineering

# **Space Systems Engineering and Operations - Final Project**

**Project Group 32**

**Professor: Lavagna Michèle Roberta**

## **Authors:**

Lorenzo Barbieri - 10702829

Riccardo Belgi - 10616718

Gaia Trovatelli - 10582310

Pietro Communara - 10676981

Mina Baniamein - 10627453

Academic Year 2022/2023

# Contents

<b>1</b>	<b>Mission Objectives, Functionalities and Mission Analysis</b>	<b>1</b>
1.1	High Level Goals . . . . .	1
1.2	Drivers . . . . .	2
1.3	Functional Analysis . . . . .	2
1.4	Phases . . . . .	3
1.4.1	ConOps link . . . . .	3
1.5	Payload analysis . . . . .	4
1.5.1	Goal-to-Payload correlation . . . . .	5
1.5.2	Payload-to-ConOps connection . . . . .	6
1.6	Preliminary MA Understanding . . . . .	6
1.7	Trajectory Design and $\Delta V$ budget . . . . .	6
<b>2</b>	<b>Propulsion Subsystem</b>	<b>9</b>
2.1	$\Delta V$ breakdown and Propulsion Choices . . . . .	9
2.2	Reverse engineering . . . . .	10
2.2.1	Propellant selection . . . . .	10
2.2.2	Propellant mass . . . . .	11
2.2.3	Pressurant selection . . . . .	12
2.2.4	Tanks sizing . . . . .	13
2.2.5	Thruster configuration . . . . .	13
2.2.6	Feeding strategy and positioning . . . . .	14
<b>3</b>	<b>Tracking, Telemetry and Telecommand Subsystem</b>	<b>16</b>
3.1	Architecture of MetOp-A's TTMTTC subsystem . . . . .	16
3.2	TTMTTC solutions and rationale . . . . .	17
3.2.1	Operations/Phases . . . . .	17
3.2.2	Data Volume . . . . .	17
3.3	Reverse Engineering . . . . .	17
3.3.1	Ground station selection . . . . .	17
3.3.2	Frequency and band selection . . . . .	18
3.3.3	Data-rate and signal manipulation . . . . .	18
3.3.4	Antenna selection . . . . .	19
3.3.5	Link budget . . . . .	20
<b>4</b>	<b>Attitude and Orbit Control Subsystem</b>	<b>23</b>
4.1	Control modes . . . . .	23
4.2	Sensors selection . . . . .	25
4.3	Actuators selection . . . . .	25
4.4	Reverse sizing . . . . .	26
4.4.1	Satellite dimensions and Inertia matrix . . . . .	26
4.4.2	Disturbances effects . . . . .	27

4.4.3	Attitude sensors sizing and pointing budget . . . . .	27
4.4.4	Attitude actuators sizing . . . . .	28
<b>5</b>	<b>Thermal Control Subsystem</b>	<b>30</b>
5.1	TCS solution identification, rationale, justification . . . . .	30
5.1.1	PLM TCS . . . . .	30
5.1.2	SVM TCS . . . . .	31
5.1.3	Thermal heat sources during the mission . . . . .	31
5.1.4	Temperature intervals . . . . .	31
5.2	Reverse engineering . . . . .	32
5.2.1	Thermal fluxes . . . . .	32
5.2.2	Hot and cold case identification . . . . .	33
5.2.3	Heat powers . . . . .	34
5.2.4	Control strategy . . . . .	35
5.2.5	Selected materials and subsystem budgets . . . . .	35
5.2.6	Subsystem layout . . . . .	36
<b>6</b>	<b>Electric Power Generation and Storage Subsystem</b>	<b>37</b>
6.1	System Architecture . . . . .	37
6.1.1	Solar Array . . . . .	38
6.1.2	Batteries . . . . .	38
6.1.3	Power Regulation . . . . .	38
6.2	Reverse Sizing - Solar Array . . . . .	39
6.2.1	Power request . . . . .	39
6.2.2	Solar cells . . . . .	41
6.2.3	Power at BOL . . . . .	41
6.2.4	Power at EOL . . . . .	41
6.2.5	Surface and mass . . . . .	41
6.2.6	Refined sizing . . . . .	42
6.3	Reverse Sizing - Batteries . . . . .	42
<b>7</b>	<b>Configuration of Space Segment</b>	<b>44</b>
7.1	MetOP-A's CONF . . . . .	44
<b>8</b>	<b>On-Board Data Handling Subsystem</b>	<b>48</b>
8.1	System Architecture . . . . .	48
8.2	Reverse Sizing . . . . .	49
8.2.1	OBC features . . . . .	49
8.2.2	On-board memory size . . . . .	51

# List of Figures

1.1	<i>MetOp A</i> . . . . .	1
1.2	<i>Chronology of activities</i> . . . . .	5
1.3	<i>Altitude (red), inclination (green) and LTAN (blue) evolution over time.</i> . . . .	7
2.1	<i>MetOp thruster configuration and location</i> . . . . .	15
3.1	<i>Frequency and data-rate</i> . . . . .	17
4.1	<i>MetOp-A's out-of-plane manoeuvre sequence</i> . . . . .	25
4.2	<i>Speed (<math>\omega</math>) vs. Torque (<math>M</math>) for a generic reaction wheel.</i> . . . .	26
4.3	<i>Thrusters positioning in MetOp-A</i> . . . . .	28
7.1	<i>Fairing dimensions</i> . . . . .	45
7.2	<i>MetOp-A engines disposition</i> . . . . .	46
7.3	<i>MetOp-A payload distribution</i> . . . . .	46
7.4	<i>Line drawing of the MetOp-A spacecraft</i> . . . . .	47

# List of Tables

1.1	<i>Inclination changing of all the six correction manoeuvres performed</i> . . . . .	8
2.1	<i>Mono-propellants performance</i> . . . . .	11
2.2	<i><math>\Delta V</math> required for each inclination correction</i> . . . . .	11
2.3	<i>Dimension and mass of MetOp-A's tanks</i> . . . . .	13
2.4	<i>Thrusters configuration and function</i> . . . . .	14
4.1	<i>List of MetOp-A attitude sensors.</i> . . . .	28
6.1	<i>Power demand</i> . . . . .	40
8.1	<i>OBDH functions of ADCS</i> . . . . .	49
8.2	<i>OBDH functions for PS</i> . . . . .	50
8.3	<i>OBDH functions for EPS</i> . . . . .	50
8.4	<i>OBDH functions for TCS</i> . . . . .	50
8.5	<i>OBDH functions for TTMTTC subsystem</i> . . . . .	50
8.6	<i>OBDH functions for satellite's operative system</i> . . . . .	50
8.7	<i>Total throughput needed by each subsystem during different modes</i> . . . . .	51

# Chapter 1

## Mission Objectives, Functionalities and Mission Analysis

*MetOp A* is the first of the series of three polar orbiting satellites in the Meteorological Operational satellite program (*MetOp*), a collaboration between *ESA* and *EUMETSAT* which represents the most contributing satellite system in acquiring data for weather broadcasting and climate monitoring and the first one to be implemented by Europe in a polar orbit. Its importance is made possible by the extremely vast and groundbreaking technology on board, which allows to undertake scientific gathering of several variables determining our climate in every single point of the planet.



Figure 1.1: *MetOp A*

Being launched in October 19, 2006, the satellite was declared fully operational in mid-May of 2007 and its expected mission operational lifetime was around 5 years, until its complete substitution with the *MetOp B* successor. Nonetheless, thanks to the precise injection in the orbit by the the Fregat kickstage, thus a minimum required correction of the orbit, the optimized strategy for the orbit maintenance and the high interest in keeping operational both *MetOp A* and *B* for redundancy and coverage reasons, the satellite was kept still operating in good health with acceptable performances till November 2021, after 15 years of service, when the orbit perigee was lowered from 817 km to about 530 km. Since then the satellite has been continuously in an orbit decay and its return to the Earth is foreseen to be within 25 years, in accordance with the international standards for the space debris mitigation.

### 1.1 High Level Goals

Overall the goal of the mission consists in gathering data using all its avantguard scientific instruments for weather forecasting, climate monitoring, environmental and space weather monitoring. For sure the most important goal is to provide accurate and timely data such as temperature, humidity and wind speed, which then are going to be used for weather forecasts. Thus is required from the satellite to provide a continuous broadcast of its meteorological data to the worldwide user community, so that any ground station in any part of the world can receive updated regional data when the satellite passes over that receiving station. And this has to be done in a specific time of the day.

The *MetOp* satellites also play a crucial role in monitoring the Earth's climate. By collecting

data on a wide range of atmospheric variables over an extended period, the mission helps scientists to track changes in the climate and understand their impact on the planet. In addition to these the MetOp mission supports a range of other environmental monitoring applications. For example, the satellites can be used to track the movement of ocean currents, monitor changes in ice cover, and detect forest fires, volcanic activities and other natural disasters. It is quite obvious that to satisfy such a demanding requirement a full coverage of the Earth, including the poles, has to be reached. Among the scientific payload *MetOp A* is also hosting multiple instruments to monitor space weather, such as solar flares and coronal mass ejections. This information is used to predict and mitigate the impact of space weather on Earth's communication and navigation systems. For this further goals different instruments have different swath widths and hence take different times to observe the entire Earth. However, all the instruments achieve almost complete global coverage within five days. All global data shall be provided to users within 2.25 hours after being taken.

A secondary mission goal was stated during the design: during the de-orbiting the satellite performed a manoeuvre in which it flipped upside-down so that the instruments would be scanning the deep space to achieve information about the space environment.

## 1.2 Drivers

Like any complex space mission, the MetOp A mission operates under a set of constraints that limits its capabilities and operational parameters. The majority of them are a consequence of the mission's main goal: the necessity of gathering as much information as possible regarding the atmosphere and of providing broadcast services to the worldwide users. The amount of science and operations which can be done are then strictly limited by number of instruments brought on the satellite and, of course, the amount of time it can be operational. Thus, the two main drivers of the mission become respectively the mass budget, which depends on the launcher service, and the lifetime of the spacecraft.

Using many sophisticated on board instruments which often require some particular conditions for nominal proper working and, of course, for their own safety, might have an effect on the main design choices. For example the ASCAT imposes a very strict constrain of frozen eccentricity maintenance, while the GOME instrument requires a constrain on the LTAN. The number of possibilities in terms of orbit selection becomes very small because a quasi polar sun-synchronous orbit shall be adopted, which allows acquiring data also from the poles but at the same time affects negatively the temporal resolution of the data, since the passage over a specific point on Earth happens once a day.

Since there's a very high number of instruments, thus of operations to be done simultaneously, a relatively high power budget is requested, which can be considered a driver. Having for example a larger solar panel on the satellite also implies higher mass to be dedicated to it, thus falling again into the limited scientific payload driver.

Also the transmitting power can become troublesome, since the bandwidth of the satellite's communication subsystem is limited and the rate of data to be sent is relatively high, representing also a further possible mission driver.

## 1.3 Functional Analysis

To reach the final goal, specific functions have to be performed:

- Reach the prescribed orbit, and check the proper working of all instruments on board;
- Be able to compute the attitude determination;

- Orient itself pointing nadir;
- Be able to correct the orbit using its propulsive system;
- Acquire data from various sensors;
- Traduce data collected by sensors into scientific informations and store them, waiting to be sent down to Earth, in the case of global data or directly transmit, in case of regional broadcast informations;
- Generate enough power to satisfy all the instrument requirements;
- At the expected end of the mission, check if all instruments on board are working well enough to give the possibility to extend mission lifetime;
- Provide an efficient solution for de-orbiting without colliding with any other satellite.

## 1.4 Phases

After detaching from the Fregat launcher upper stage the satellite entered the so called LEOP. It must be underlined that this phase does not enter into the jurisdiction of EUMETSAT, thus the satellite is still in total control of the launcher company. LEOP (Launch and Early Orbit Phase) is the phase in which the solar array and the antennas are deployed. The first in-orbit correction manoeuvres were performed as well at the end of an automated sequence that initialized in-orbit operations.

Following the LEOP handover, the SIOV (Satellite In-Orbit Verification) phase began on October 23, 2006 and lasted all the way up to March 29, 2007. The main objective of the SIOV was to dedicate a specific period where the performance and functionality of the satellite was verified in-flight. For this reason SIOV will systematically switch on all of MetOp's functions and verify the performances of the Service Module, Payload Module and instruments. While in SIOV, the first instruments that were turned on and began their operations were ASCAT and GRAS.

Once the MetOp satellite was verified in orbit, the Verification and Validation of the full Eumetsat Polar System (EPS) began. In this phase it was performed an end-to-end check of the functionality and performance of the instrument chain from the data acquisition on board to the generation of the high level products. The verification and validation of the chain was also done to calibrate the instruments using real data.

The satellite was declared functional on May 15, 2007 thus ending its disposal phase. Then the Start Of Regular Operations (SORO) began. At this point calibrations were still ongoing.

The EOL (End of Life) phase was designed to be around 2015 but as the satellite performed above the original expectations this phase was pushed back all the way to 2021 [Figure 1.2].

### 1.4.1 ConOps link

There are different ConOps for each phase of the mission:

**SIOV** During this phase the main goal was to validate all on-ground and on-board equipment and functions to ensure their full readiness. FDF (Flight Dynamics facility) operations were performed in the server according to the nominal routine operation scheme:

- Once a day: orbit determination and orbit product generation;
- Twice a day: OBTUCT correlation and SVM TCH generation;
- Once a day: HKTM processing.

After one week of manual operations, needed to validate the reliability of the system and to accumulate a batch of enough CDA data, automatic operations were started: manual check of products before distribution was however maintained. Moreover, dedicated campaigns were carried out to assess the readiness of the back-up units.

**EPS-IO-V&V** During the Verification and Validation phase the main goal was the monitoring of the quality of the products against the mission requirements; that implies to assess the accuracy of:

- Orbit determination and propagation;
- OBTUTC correlation;
- Satellite pointing;
- AOCS TCH;
- Geometric and vector products.

Operations needed to continuously perform these monitoring activities during routine. Dedicated analyses were performed to characterize the generation processes in terms of minimum data amount needed for the estimation processes and optimal configuration for AOCS TCH and vector products generation. Other analyses were focused on further investigation of the problems identified in the SIOV.

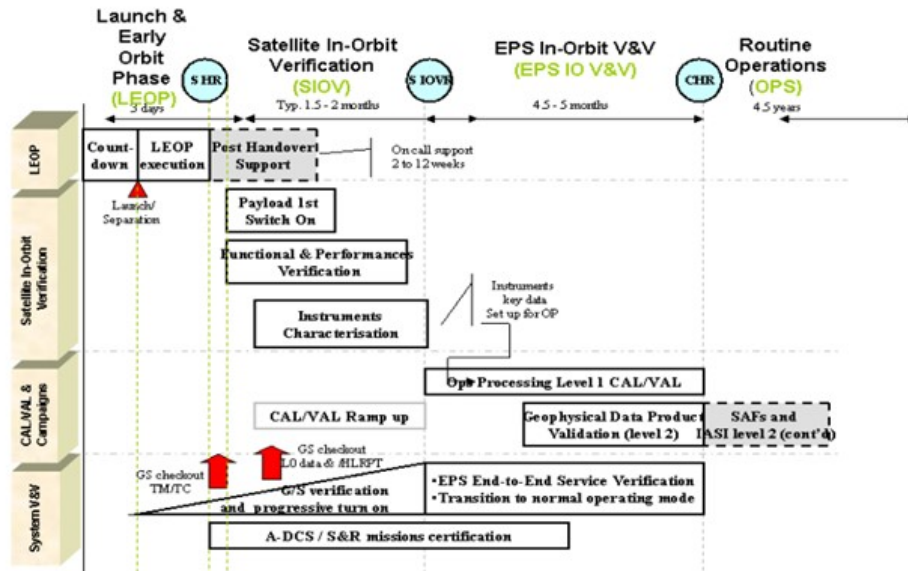
**Routine operations** During routine operations a continuous monitoring of all Flight Dynamics functions, based on the monitoring activities developed in SIOV and V&V, is performed. That ensures the maintenance of the achieved performances. Furthermore, standard activities of monitoring of the orbital evolution and implementation of orbital maintenance manoeuvres are carried out. The generation of routine products needed for fulfilling the FDF mission requirement is performed in the server according to the following operational drivers:

- 3 operational sequences are executed daily to fulfil with the need of updating the SVM TCH twice a day and to update the mission planning and GRAS support network (GSN) products once a day;
- Events for mission planning are generated weekly and re-synchronised daily to the latest values of the ascending node crossing time;
- SVM TCH must be generated considering geocentric pointing and not considering any manoeuvre in the future up to the day of the manoeuvre itself;
- Mission planning and GSN products are generated considering estimated attitude (nominally Yaw Steering Mode - YSM) and manoeuvre prediction 3 days in the future.

## 1.5 Payload analysis

The payload of the MetOp-A satellite consists of a total of 13 scientific instruments for meteorological observation carried by the Payload Module (PLM). The 13 instruments on-board are: MHS, AVHRR/3, A-DCS3, S&R (NOAA), SEM (POES), AMSU-A, GOME-2, GRAS, ASCAT, HIRS/4, IASI.



Figure 1.2: *Chronology of activities*

### 1.5.1 Goal-to-Payload correlation

The function of each instrument of the PL will be briefly discussed in the following section.

ASCAT is an active ESA instrument. Objective: Determining wind vector fields at sea surface by measuring the back-scattering coefficient [normalized radar cross section sigma-nought ( $\sigma^0$ ), also referred to as NRCS] on a global basis. The requirement calls for the measurement of wind speeds in the range of 4-24 m/s with an accuracy of 2 m/s and a direction accuracy of  $\pm 20^\circ$ . In addition to measuring wind vectors, ASCAT will also help monitor snow and ice distribution over land and sea.

MHS is a five-channel self-calibrating instrument, providing humidity profiling capability in the frequency range of 89 - 190 GHz. The channels 2-5 provide a humidity sounding capability (water vapor absorption line), while channel 1 measures the Earth's surface temperature and emissivity, in conjunction with the AMSU-A window channels, and detects cloud and precipitation contaminated pixels. The MHS instrument is a total power radiometer which measures the total noise power from the scene.

IASI is designed to measure atmospheric spectra in the infrared. It comprises a Fourier transform spectrometer (FTS) and an associated imager.

GOME-2 measures the solar radiation transmitted or scattered from the Earth's atmosphere or from its surface. It measures the total column amounts and stratospheric and tropospheric profiles of ozone. GOME can also be used to investigate the distribution of atmospheric aerosols and clouds-plus-surface spectral reflectance.

GRAS provides atmospheric temperature and humidity profiles.

The primary objective of A-DCS3 is the collection and dissemination of data for the scientific community, through the measurement of temperature, pressure, humidity, sea levels and location.

The S&RSAT payloads are part of an international cooperative satellite-based radio-location system (COSPAS-S&RSAT) to support search and rescue operations for aviators, mariners, and land travellers in distress.

SEM-2 is a spectrometer that provides measurements to determine the intensity of the Earth's radiation belts and the flux of charged particles at the satellite altitude. It provides knowledge of solar terrestrial phenomena and also provides warnings of solar wind occurrences that may impair long-range communication, high-altitude operations, damage to satellite cir-

cuits and solar panels, or cause changes in drag and magnetic torque on satellites.

### 1.5.2 Payload-to-ConOps connection

An 18 months control-free time window was considered after launch. In this window the satellite tested all the different on-board instruments and performed a first series of orbit correction manoeuvres. After this phase was completed the instrumentation was turned on and begun nominal working.

As before mentioned a continuous series of correcting manoeuvres is made constantly to keep the satellite on the best possible orbit (within a nominal error range) in order to collect the best possible scientific data and to maximize the ability of the satellite to communicate with the GS.

## 1.6 Preliminary MA Understanding

As already mentioned a nearly polar sun-synchronous and circular orbit is required for this mission, as a constraint imposed by the payload instrumentation. MetOp-A flies at an altitude of 824 km with an orbital inclination of 98.7°. The orbital period of these satellites is 101.4 minutes with a 14-day repeat cycle.

Being on a sun synchronous orbit means that the the combination of inclination and altitude is chosen in a way that the orbit's precession follows the rotation of the planet around the Sun and as a consequence the satellite passes above each point of the planet at the same local time during the whole year. This is quite an important feature for a satellite whose objective is to transmit broadcast information to all the users on the planet at a specific time of the day. Hence the MetOp-A was intended to be a morning service satellite while the cooperating NOAA satellite system would cover the broadcast transmitting during the afternoon.

A sun synchronous orbit can be very useful for certain aspects. For example, during the orbit the variation of the relative direction of the Sun while the spacecraft is pointing nadir is limited. Thus the spacecraft geometry and the positioning of components, such as payload, solar panels, radiators, attitude determination sensors, can be designed in a very efficient way.

One of the design choices of this mission is to achieve a repeated ground track every 29 days with a dead band error of 5 km. In this way the monitoring of the same places can be done monthly. Since the swath width of the IASI instrument is in the range of Since this is imposing a constraint on the semi major axis then also the inclination is fixed. The selection of the orbit parameters mentioned above have also been made in a way to make the on-board instruments of the payload work all in their optimal range of operations, as anticipated in the 'Drivers' chapter. The definition of the nominal orbit is also made as a trial to minimize the eccentricity drift away to 0.00003 or less, since a higher value would require more complex calibration for the ASCAT instrument. Another choice for the mission which has been made for satisfying the operating conditions of the payload is the manoeuvring during the eclipse only, since of many them cannot be illuminated directly by the Sun. On the other hand local time of the ascending of 09:30 reduces the sun glint and provides sufficient Earth illumination for the optical instruments.

## 1.7 Trajectory Design and $\Delta V$ budget

MetOp-A was loaded with approximately 316 kg of hydrazine at launch. This amount of fuel was budgeted for orbit maintenance, for correction of orbit injection errors following separation

from the launcher and to maintain the satellite in a safe attitude in case of a major anomaly at platform level.

A first, rough estimation of the  $\Delta V$  budget can be obtained through Tsiolkovsky rocket equation. It shall however be pointed out that for the type of manoeuvres considered for the MetOp-A mission this is not the best estimations as the hypothesis of an impulsive manoeuvre is not verified.

The specific impulse  $I_{sp}$  is roughly 220s; the initial mass is 4085kg and the fuel mass is 316kg. The efficiency of the PS can be assumed to be around 93.1%, thus the rocket equation can be written as:

$$\Delta V = g_0 \eta I_{sp} \ln\left(\frac{m_i}{m_f}\right) \quad (1.1)$$

The end result is a  $\Delta V$  of roughly 163 m/s.

No fuel was initially allocated to de-orbiting, since no End-of-life (EOL) disposal was imposed at design time. During its first 7 years of operational life a large amount of fuel has been saved in comparison with the design case. Around 208 kg of hydrazine were estimated to be still onboard at the beginning of 2014; out of these, 198 kg are considered to be still usable. The orbit control is achieved by the execution of two types of manoeuvres:

- In-plane (IP) manoeuvres to change the semi-major axis (and eccentricity) which allow to control the ground track deviation
- Out-of-plane (OOP) manoeuvres to correct the inclination, allowing to control the drift of the ascending node and its local time.

From graph below it is possible to write down all the differences in the inclination of the orbit for each OOP manoeuvre and to understand that the evolution of LTAN is continuous, meaning that during the impulse it is not being changed (the manoeuvre is centered on the equator). In 7 years six corrections for the inclination have been done [Figure 1.3].

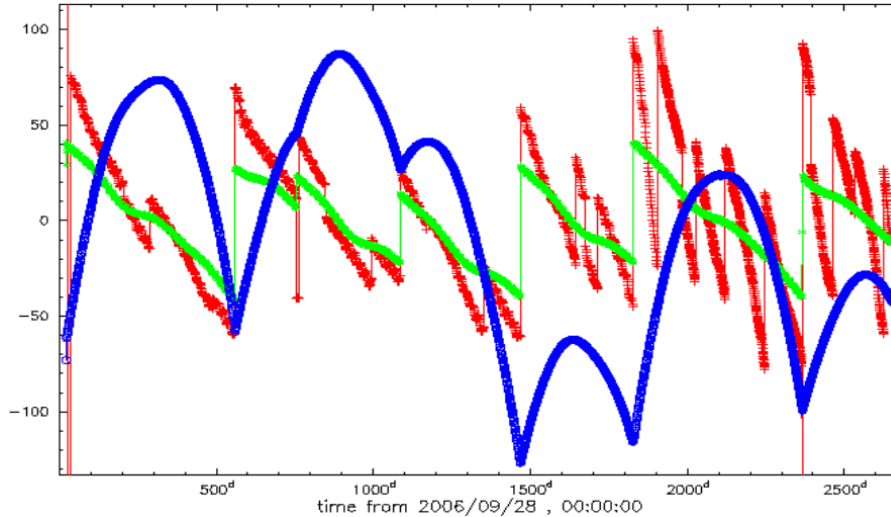


Figure 1.3: *Altitude (red), inclination (green) and LTAN (blue) evolution over time.*

$$\Delta V = 2V \sin \frac{\Delta i}{2} \quad (1.2)$$

The  $\Delta V$  for each of those impulses can be computed, using the formula above, and by making the sum of all the results a final required  $\Delta V$  for the inclination correction is obtained: 40 m/s, corresponding to 76 kg of fuel. The same procedure can be done for the correction of

<i>Initial i deviation</i> [deg]	-48	9	-23	-40	-11	-39
<i>Final i deviation</i> [deg]	28	22	13	28	40	22
$\Delta i$ [deg]	76	13	36	68	51	61

Table 1.1: *Inclination changing of all the six correction manoeuvres performed*

the semi-major axis. However a much more simplified model is being used, in order to obtain just an approximation of the  $\Delta V$  budget for this type of manoeuvre.

One of the simplification is dealing with only circular orbits and correcting the altitude by undertaking a simple Hohmann manoeuvre. Since both the altitudes at the beginning and at the end are given in the graph from before, the amount of total  $\Delta V$  is immediate to compute, resulting in just 1.55 m/s (2.94 kg of burnt fuel).

It is important to consider also the amount of fuel spent for each slew manoeuvre, for which the reference (1) indicates it is around 1.3 kg of hydrazine. In the same document the adopted strategy for the distribution of manoeuvres along the satellite's lifetime is explained, being also the one which is represented in figure 1.3. For each campaign during the autumn equinox 2 correction manoeuvres are needed, while for the smaller manoeuvres during spring equinox one single burn is enough. From this it follows that during the first 7 years a number of 11 inclination correction manoeuvres are being undertaken, corresponding to about 14.3 kg of fuel. In the reference (6) it is told that during the design an amount of 60 kg of fuel is allocated to the acquisition of the orbit, and from those only 11.6 are being used. By doing the sum of all the masses of fuel spent in the operations explained above, it is possible to justify the  $\Delta V$  spent during the mission and to compare it with the total  $\Delta V$  budget of the mission.

The computed total mass spent is equal to 105.76 kg. According to the documents 108 kg of hydrazine are being burnt during these year, and they are well justified by the 105.7 kg result from the calculations. The equivalent  $\Delta V$  which can be retrieved by the mass is around 56.6 m/s, well below the  $\Delta V$  budget of 163.5 m/s. The remaining fuel was then used to extend the mission duration by many years.

However an amount of 157 kg of fuel has been saved in order to bring the satellite to a lower orbit, with a perigee around 600 km. This way it is possible to achieve an orbit decay within the admitted 25 years term.

## Chapter 2

# Propulsion Subsystem

MetOp-A is a satellite dedicated to operational meteorology and it has a near-circular sun-synchronous polar morning orbit, therefore the propulsion system has to assure just one primary maneuver: the insertion into this specific orbit. This maneuver, that correspond to the LEOP phase, is controlled by the launcher company but it's performed by the same propulsion system as the following secondary maneuvers; for this reason it must be as well considered for the  $\Delta V$  breakdown. After this first orbital correction, the only maneuvers that occurs are those of station-keeping and attitude control; they remain the same for each of the consequent phases of SIOV, V&V and RO, as the change of phase only impact the data analysis and not the satellite positioning.

As anticipated in the previous assignment, the orbit control is achieved by the execution of two types of maneuvers:

- In-plane (IP) manoeuvres to change the semi-major axis (and eccentricity), which allow to control the ground track deviation
- Out-of-plane (OOP) manoeuvres to correct the inclination, allowing to control the drift of the ascending node and its local time.

Thanks to the high redundancy of propellant, that was not utilized for the correction of errors, and the still optimal performances of the satellite, the duration of the mission was extended of several years, reaching 11 years of nominal operational life. From June 2017 MetOp-A was exploited on a "drifting" orbit in order to further extend its useful lifetime from 2019 to 2022. It was however decided to not perform anymore the inclination correction, due to its high cost, and the local time at ascending node decreased in time from the nominal mission value.

In the end, because thermal constraints imposed by MetOp-A drift made it difficult to guarantee the safety of the spacecraft in the winter of 2021-2022, EUMETSAT opted to de-orbit MetOp-A to a lower perigee orbit for reentry. The EOL (End of Life) is expected for December 2027.

These final maneuvers were not initially considered in the mission design and were added in a second time.

## 2.1 $\Delta V$ breakdown and Propulsion Choices

The architecture of the propulsive subsystem in the MetOp-A is composed by a set of eight hydrazine based mono-propellant blow-down architecture engines, designed to provide at the beginning of the satellite's life a thrust of 22.7 N.

The determination of the propulsion subsystem is strictly dependent on the amount of  $\Delta V$  to be imposed on each manoeuvre and on the limited time in which the impulse has to take place. Since the manoeuvre has to be done within the eclipse, which only lasts a few

minutes, it is clear that the amount of time is very limited for the thrust process. Either the propulsive subsystem has to achieve the full correction in that small amount of time, or the orbit correction has to be done with multiple impulses. It is very important to consider for a mono-propellant engine that the available thrust level of the engines decreases in time. Thus the number of impulses for one orbit correction campaign might increase in the end. In the previous assignment it has been seen that the satellite should be able to provide a change in  $\Delta V$  to provide a 78 *mdeg* attitude correction in the worst case. By assuming that:

- during one single correction manoeuvre the variation of the spacecraft's mass can be considered negligible;
- The duration of the eclipse is varying during the year and its lowest value is around 7 minutes;
- During the lifetime each campaign requires a maximum number of 2 correction manoeuvres;

It is possible to estimate the required acceleration using these values, since the change in velocity is given by acceleration times burning time, and the plane change formula. For this the absolute value of the velocity in circular orbit can be easily obtained (7.44 km/s). Thus, the  $\Delta V$  and the acceleration needed are respectively 5.064 *m/s* and 0.00804 *m/s<sup>2</sup>*. The available acceleration given by the two implied engines can be obtained instead by their thrust and the satellite's mass using Newtons equation. For this the values are taken at end of life, that it is the worst case scenario. The result obtained is 0.00928 *m/s<sup>2</sup>*, which is in range with the previous number, then the selection of this value for the thrust is justified.

From this point of view it can be understood that the mono-propellant system might be a good choice, since it usually provides a quite large range of thrusts, from less than one Newton up to one hundred. Bi-propellant rocket engines also can provide levels of thrust in the same range but they are much more complex to design, in terms of feeding, pressurizing and cooling system, implying not only more inert mass, but a significant increase in both cost and complexity as well. They are also less throttleable and they always require an ignition system to restart the engine, thus they are not the most suitable option for an engine that has to be restarted multiple times. On the contrary, a mono-propellant rocket engine does not require this and can be reignited unlimited times. Cold gas engines are also very easy to deal with in multiple manoeuvres missions but the thrust they can give is too limited for this case and they are usually implied in attitude control only. Their specific impulse is also much lower than mono-propellant's.

## 2.2 Reverse engineering

### 2.2.1 Propellant selection

Hydrazine is a very interesting mono-propellant as it has two major features that make it a good, suitable choice for the job. Even though hydrazine is a highly toxic molecule and requires a very specific skill set of abilities to be handled (making it both expensive and exotic to use) it benefits of both a lower density and a lower combustion temperature, compared to the average of the mono-propellants. Furthermore hydrazine has been the state of the art for almost 70 years and no other propellants have been intensively studied in the space environment. Among them the ionic propellant families HAN and ADN represent the possible candidates for future-generation mono-propellants, being much less toxic and superior in performance than hydrazine. At present their behaviour in space is still unknown while the hydrazine holds a very large heritage, and this is the reason why it is very common-use to rely on it.

Property-Fuel type	H <sub>2</sub> O <sub>2</sub>	N <sub>2</sub> H <sub>4</sub>	N <sub>2</sub> O
Density [ $\frac{Kg}{m^3}$ ]	1388	1020	1977.7
Specific Impulse* [s]	160	191	152.7
Combustion temperature [K]	1274	896	1609

Table 2.1: *Mono-propellants performance*

In this table the  $I_{sp}$  was computed with a chamber pressure of 7 bars and an area ratio of 40, this is why it is different from the 220s value declared above. This means that hydrazine can provide a good specific impulse (the engines on the MetOp-A have roughly a  $I_{sp}$  of 220s) while making it relatively easy to cool the engine, not adding extra weight for specific cooling devices. Hence the chamber temperature around 1000 K of hydrazine is relatively low with respect to other mono-propellants and much lower with respect to bi-propellant combustion.

### 2.2.2 Propellant mass

The sizing of the propellant mass can be driven by the initial total dry mass at launch and by the required  $\Delta V$ . In the last report it has been seen that an amount of 55.6 m/s have been used for the orbit maintenance in the first 7 years, roughly the predicted lifetime of MetOp-A. Among this, 6.14 m/s of  $\Delta V$  was spent for the orbit injection after the decoupling from the launcher stage, 40.25 m/s were used for the OOP manoeuvres and around 1.55 m/s for the eccentricity and altitude maintenance.

	i change 1	i change 2	i change 3	i change 4	i change 5	i change 6
$\Delta V$	10.1278	1.9476	4.6744	8.8293	6.6220	8.0503

Table 2.2:  $\Delta V$  required for each inclination correction

Since these are deterministic accurately calculated manoeuvres a margin of 5% of the sum or 10 m/s shall be applied at the design; in this case it has been considered the second option since it's the highest value, therefore more conservative. Same thing has to be done for the IP manoeuvres. For the initial orbit correction, being a stochastic manoeuvre which depends on the launcher injection, a 100% margin shall be applied to the assigned  $\Delta V$ . Thus the total  $\Delta V$  required for each type of manoeuvre is:

- 50.25 m/s for OOP;
- 11.5 m/s for IP;
- 12.28 for orbit injection;

resulting in 74.03 m/s total  $\Delta V$  for the mission. The total dry mass at launch can be obtained by adding a 20% margin to the nominal dry mass (3769 kg) and it is equal to 4523 kg. By using Tsiolkovsky equation it is possible to obtain the required propellant mass: 158.78 kg. At this point some corrections to nominal propellant mass shall be applied. In particular, it must be added 3% of propellant to take into account ullage, another 2% for residuals, according to **MAR-MAS-080**, and 0.5% for loading uncertainties. That leads to a real propellant mass of 166.5 kg.

Knowing the density of hydrazine ( $1010 \text{ kg/m}^3$ ), it can then be computed the volume of propellant, that is  $0.165 \text{ m}^3$ . Once again, it must be considered a 10% margin of unusable volume (**MAS-CP-010**), and so the final propellant volume becomes  $0.181 \text{ m}^3$ .

### 2.2.3 Pressurant selection

The most common gases used for pressurant purposes are helium and nitrogen.

Helium is often used as a pressurant gas due to its unique physical and chemical properties. As a noble gas, helium is non-reactive and does not easily form compounds with other elements, making it a safe and reliable choice for pressurization applications.

One of the primary advantages of helium as a pressurant gas is its high volumetric efficiency. This means that a relatively small amount of helium can be used to achieve a high pressure, making it a cost-effective option for many applications.

Helium is also chemically inert, meaning it does not react with other substances. This makes it a safe choice for use with sensitive materials or in environments where contamination could be a concern.

Another advantage of helium is its high thermal conductivity, which allows it to dissipate heat quickly. This property is particularly useful in applications such as cryogenics, where maintaining low temperatures is critical.

Overall, helium is an excellent choice as a pressurant gas due to its low density, chemical inertness, and high thermal conductivity. It is used in a wide range of applications, including rocket propulsion, welding, and leak detection, among others. Nitrogen is also commonly used as a pressurant gas due to its unique properties. Nitrogen is an inert gas, meaning it is non-reactive and does not readily form compounds with other elements. This makes it a safe and reliable choice for pressurization applications.

One of the primary advantages of nitrogen as a pressurant gas is its availability and low cost. Nitrogen is abundant in the Earth's atmosphere, and it can be easily separated from other gases using a process called air separation. This makes it a cost-effective option for many applications. Another advantage of nitrogen is its low reactivity, which makes it a safe choice for use with sensitive materials or in environments where contamination could be a concern.

However, nitrogen does have some limitations as a pressurant gas. It has a lower thermal conductivity than helium, which can make it less effective in applications where heat dissipation is critical. Nitrogen can also support combustion in certain conditions, so it may not be suitable for use in environments where flammability is a concern. Compared to helium it has a lower density, making it less suitable for a weight save, which is necessary in order to allow more payload mass, or fuel mass orbit maintenance requirements. Therefore the most suitable pressurant for the mission is helium.

Starting from an initial helium pressure of 22 bar, and assuming a final gas pressure of 5.5 bar, the minimum value of feed pressure that the engines can work at, it is found immediately the blow-down ratio  $B$ , equal to 4. This value is acceptable, because most of the satellites with this propulsion architecture have a blow-down ratio between 4 and 6. Once known  $B$ , the initial volume of pressurising gas can be computed with an isothermal transformation.

$$V_{gas,i} = \frac{V_{prop}}{B - 1} \quad (2.1)$$

Initial helium volume is  $0.061 \text{ m}^3$ .

Next step is the evaluation of gas mass with the ideal gas law, knowing helium gas constant,  $R_{specific} = 2077.3 \frac{\text{J}}{\text{kgK}}$ , and  $T = 293 \text{ K}$ :

$$m_{gas} = \frac{P_{gas,i} V_{gas,i}}{R_{specific} T_{gas}} \quad (2.2)$$



The final helium mass is 0.262 kg, obtained after adding 20% margin (**MAR-MAS-090**) to  $m_{gas}$ .

### 2.2.4 Tanks sizing

All the on board propellant is stored in four independent tanks, coupled in pairs. Each pair of tanks supplies hydrazine to eight thrusters. During normal operation phases, both tank pairs are in use. Total tank volume is 0.244 m<sup>3</sup>, obtained by the sum of helium and propellant volumes, plus 1% margin for the bladder volume. Each single tank then has a volume of 0.061 m<sup>3</sup>, this value is necessary to determine tank dimension and mass. Assuming the shape of vessels is spherical:

$$r_{tank} = \frac{3}{4} \left( \frac{V_{tank}}{\pi} \right)^{\frac{1}{3}} \quad (2.3)$$

$$t_{tank} = \frac{P_{tank} r_{tank}}{2\sigma} \quad (2.4)$$

Where  $P_{tank}$  is equal to  $P_{gas,i}$ , and  $\sigma$  is material's ultimate stress. Finally, the mass of a single tank is:

$$m_{tank} = \rho_{tank} \frac{4}{3} \pi ((r_{tank} + t_{tank})^3 - r_{tank}^3) \quad (2.5)$$

Most widely-used materials for spacecrafts' tanks are aluminum or titanium alloy. Hereafter are presented results for both of them.

	Ti-6Al-4V	Al7075
$\rho [\frac{kg}{m^3}]$	4429	2810
$\sigma [MPa]$	950	503
$r_{tank} [m]$	0.244	0.244
$t_{tank} [mm]$	2.8	5.3
$m_{tank,single} [kg]$	9.5	11.5
$m_{tank,tot} [kg]$	38	46

Table 2.3: *Dimension and mass of MetOp-A's tanks*

It is easy to figure out that using titanium alloy would mean thinner and lighter tanks, and so this is the adopted material.

### 2.2.5 Thruster configuration

The eight engines of MetOp-A generates torque around all three axis and thrust effect along Y direction. They are mounted in pairs and are positioned in order to meet both thrust and torque levels required by the system. Thrusters number 7, 9, 13 and 15 are the so-called propulsion thrusters: they are commonly used to provide the necessary thrust in the flight direction while keeping the torque balanced. However, torque imbalance can occur during the propulsion phase due to changes in spacecraft's center of mass. The four single thrusters are instead the attitude control thrusters: they give the necessary torque to the spacecraft to stabilise the attitude pointing [Table 2.4]. A graphical view of thruster pair configuration is shown in Figure 2.1. On the left side of the picture there is a rough representation of the spacecraft body with some green patches, that stand for the location of thruster pairs on the satellite body.

Thruster N°		Thruster function	
Prime	Redundant	Torque	Thrust
1	2	+Y	
3	4	-Y	
5	6	-X	
7	8	-Z	-Y
9	10	+Z	-Y
11	12	+X	
13	14	+Z	+Y
15	16	-Z	+Y

Table 2.4: *Thrusters configuration and function*

### 2.2.6 Feeding strategy and positioning

MetOp-A works on a propellant blow-down feeding system, where the propellants are stored in high-pressure tanks and are released to the thrusters by opening a valve. The system relies on the pressure built up in the propellant tanks to force the propellants out and into the thrusters. Some potential advantages of a blow-down feeding system include simplicity and reliability, because blow-down systems are generally simpler and easier to design, construct, and operate than other types of feeding systems, as they require fewer components and mechanisms. So they do not depend on complex mechanisms or moving parts that can fail. Blow-down systems are typically lightweight and compact, as they require fewer components. This also makes it cost-effective, resulting in lower overall mission costs. The positioning of the tanks and lines on the MetOp-A spacecraft was designed to maximize the efficiency and reliability of the propulsion system while minimizing the impact on the spacecraft's overall mass and balance. The tanks are mounted on opposite sides of the spacecraft to maintain the spacecraft's balance and stability. The propulsion system is designed to be highly modular and redundant, with multiple thrusters and valves connected to the same lines and tanks to provide backup options in case of failures. Overall, the positioning of the tanks and lines on MetOp-A was carefully planned and optimized to ensure that the propulsion system functions reliably and efficiently, enabling the spacecraft to maintain its desired orbit and complete its Earth-observing mission with high accuracy and stability.

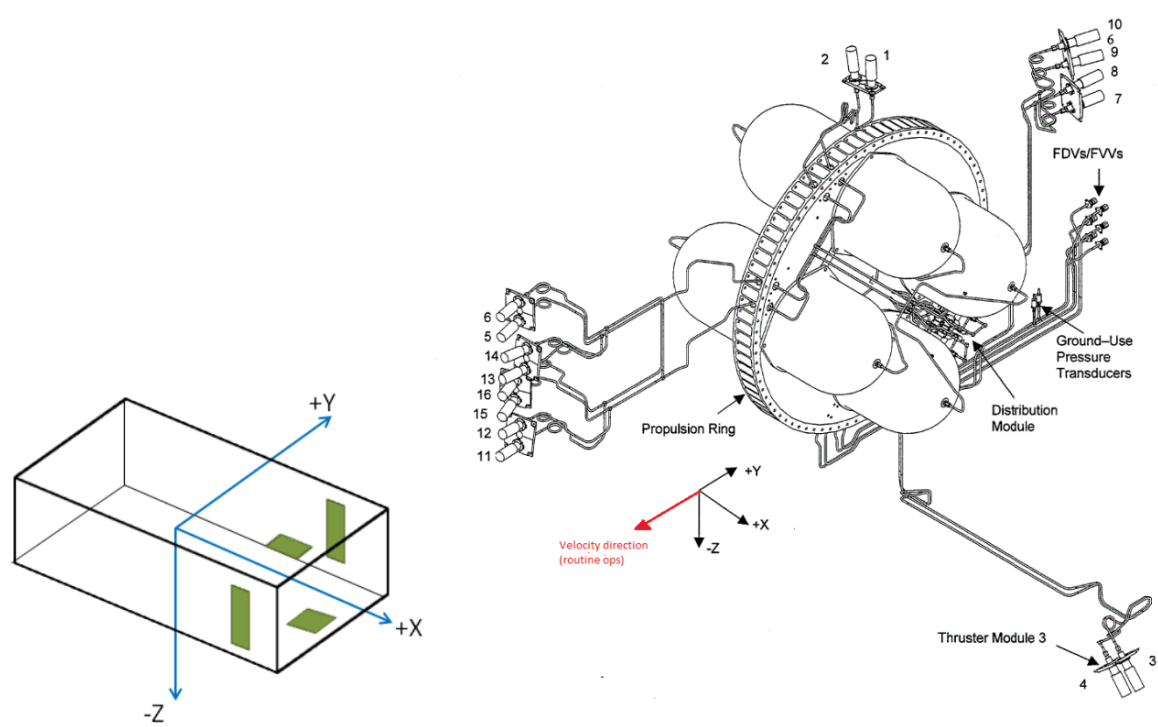


Figure 2.1: *MetOp thruster configuration and location*

## Chapter 3

# Tracking, Telemetry and Telecommand Subsystem

Change Log	
3.3.3 Data-rate and signal manipulation	Page 19: Added values for S-band data-rate.
3.3.5 Link budget	Pages 20-21: Added results for S-band up-link sizing; Page 21: Input power and antenna gain explained better.
3.3.5 Link budget	Pages 21-22: Added paragraphs on modulation index, carrier power and signal-to-noise ratio.

The TTMTC is the Telecomm subsystem and it is the one that grants communications between the satellite and the Earth. There are two directions a communication can go which are the Down-link, where the signal is sent from the spacecraft to the ground and the Up-link in which the opposite happens. These two directions usually handle different kinds of data. The Down-link handles both Engineering (telemetry) and Payload data type. Both this data can be either digital or analog. The Up-link, on the other hand, handles data such as Commands, SW patches and so on. There are 4 different autonomy levels that the spacecraft can have as stated in norm ECSS-E-ST-7011C and they range from Mission executed under ground control all the way up to Execution of goal-oriented tasks on board. TTMTC is affected by several non-optimal aspects such as losses, interferences and so on; these issues have consequences on the power and mass budgeted as typically larger, more powerful devices are required to overcome such problems.

### 3.1 Architecture of MetOp-A's TTMTC subsystem

An omnidirectional S-band coverage provides TT&C support: a telecommand up-link of 2 kbit/s and a satellite housekeeping telemetry down-link of 4 kbit/s. The science data from the instrument suite is sent to the data handling avionics in the form of data packets and their transmission to ground is ensured by three links:

- an X-band link to the CDA station at a rate of 70 Mbit/s
- LRPT and AHRPT providing continuous data transmission to ground respectively in VHF with 72kbit/s and L-bands with 3.5 Mbit/s for local users

To ensure high quality images the provided VHF low-ratio digital direct broadcast service replaces the old analog APT service of NOAA. The digital LRPT service retains the VHF frequency and bandwidth of the APT service, but provides three channels of AVHRR data at the full instrument spatial and radiometric resolution. On-board storage capacity of 24 GB, which is slightly more than one full orbit of data, is provided by the SSR (solid state recorder); it has a data rate of 70 Mbit/s.

Data Description	Frequency Domain	Useful Bit Rate
TT&C uplink	S-band 2053.4 MHz	2000 bps in NRZ/PSK/PM
TT&C downlink	S-band 2230 MHz	4096 bps in SP-L/PSK/PM
Global Data Stream downlink	X-band 7750-7900 MHz	70 Mbps in QPSK
LRPT downlink	VHF 137.1 MHz	72 kbps in QPSK
HRPT downlink	L-band 1701.3 MHz	3.5 Mbps in QPSK

Figure 3.1: *Frequency and data-rate*

## 3.2 TTMTTC solutions and rationale

### 3.2.1 Operations/Phases

The data handling for telemetry and telecommand does not vary through the different phases of the mission, while the transmission of science data from the payload only began at the end of the SIOV phase, as the instrumentation is off in the early phases and only the data for the spacecraft health monitoring are analyzed. Once the RO phase starts, as the orbits of the MetOp-A satellite are designed in such way that there are no blind orbits, the satellite is always into science mode in order to gather and collect as much data as possible.

### 3.2.2 Data Volume

The total amount of collected data can be split into two categories: telemetry and science data. The telemetry requires the transmission of a low amount of data, while there is a large amount of data-collecting payload; for this reason there are several antennas transmitting different kinds of data on the ground. The communication of the science data and the telemetry ones is kept separated. The bulk volume of the data collected can, at first, be approximated to be as big as the on-board storage system, that is 24 Gbit.

## 3.3 Reverse Engineering

### 3.3.1 Ground station selection

Command and Control of MetOp is performed from the EPS Control Room at EUMETSAT Headquarters in Darmstadt, Germany. The control center is connected to the Command and Data Acquisition (CDA), located at Svalbard Satellite Station in Norway. This high northern latitude position of 78° N benefits from the close proximity of orbit tracks at the poles and

ensures visibility and commanding by the CDA for all MetOp daily orbits (there are no blind orbits); in this way the CDA can provide TT&C coverage on each orbit. Visibility profiles allow contact periods varying between 4 and 12 minutes with a typical period of better than 10 minutes. Commands for routine operations are generally uplinked at each CDA contact, approximately 36 hours in advance of on-board execution.

This ground segment for MetOp missions was designed to achieve a worst case end-to-end timeliness for MetOp global products of 135 minutes. However, in 2010 a data acquisition service at the Antarctic was considered by EUMETSAT and its US partners, to improve products timeliness towards the end users. ADA (Antarctica Data Acquisition), an international partnership of EUMETSAT, NOAA, NASA and NSF, implemented a new capability connecting McMurdo Station (Antarctica) to EUMETSAT's Darmstadt, Germany Control Centre for the purpose of improving (decreasing) the latency of MetOp satellite data by 50%, from 130 minutes to 65 minutes. EUMETSAT declared ADA operational for MetOp on schedule in June 2011 and MetOp-A became the first polar-orbiting environmental satellite to achieve the 65-minute data latency operationally.

### 3.3.2 Frequency and band selection

The frequency selection depends on multiple factors among which there are the amount of data that has to be transmitted and the distance at which it has to be transmitted at. As the TT&C data is in the range of 4 kbps at its peak, and the distance the signal has to travel is in the range of a few thousand kilometers, S-band coverage was chosen. This allowed the use of a LGA. The science data was initially dumped once for every orbit, then, starting 2011, a second dump was introduced in order to reduce the latency by over 50 *percent*. The large amount of data that has to be dumped each time, combined with a short communicating window (4-12 minutes) meant that a higher frequency is required. X-band was chosen for these reasons.

### 3.3.3 Data-rate and signal manipulation

As previously outlined, the data volume that needs to be transmitted to the ground can be approximated to 24 Gbit. Considering the worst case scenario of visibility time, this amount of data needs to be transmitted in approximately 4 minutes; the resulting data-rate can be then easily computed:

$$R_{ideal} = \frac{V_{data}}{T_{window}} \quad (3.1)$$

The worst-case scenario data-rate is then roughly 100 Mbit/s.

Once the theoretical data-rate handled by the spacecraft is fixed in the design phase, both encoding and modulation shall be determined as they have an effect on the real data-rate of the satellite. A QPSK modulation is used for all the scientific data in order to optimize the spectrum use; the typical coefficient for this type of modulation is 2. Telemetry data is modulated with three different techniques among which the most used one is the PSK. A typical value of the modulation coefficient for PSK techniques can be found in the literature and is around 1. Typical encoding techniques for satellites rely on the Reed-Solomon encoding: which is capable of granting an encoding coefficient of 1.14 and a minimum  $\frac{E_b}{N_0}$  of 5.5 dB. Considering these modulations of the signal, the real data-rate can be adjusted according to the following formula:

$$R_{real} = R_{ideal} \frac{\alpha_{enc}}{\alpha_{mod}} \quad (3.2)$$

It shall be noticed that with the before-mentioned values for the encoding and modulation coefficients the real data-rate is lower than the theoretical one. With these values we can

obtain a real data-rate of 57 Mbit/s, that, when taking into account all the safety margins required, is reasonably close to the 70 Mbit/s selected by EUMETSAT. **Instead for what concern the transmission in S-Band through the omnidirectional-antenna the data rates are definitely smaller, with an up-link for telecommands of 2 kbit/s and a down-link of 4 kbit/s.**

### 3.3.4 Antenna selection

The selection of the antenna type depends primarily on the data-rate and frequency, but it is also important to considerate the time window. As said before, the MetOp-A has a large amount of data to transmit to ground and a visibility period with the ground station of approximately 10 minutes. The distance between the satellite and the ground station stays the same during the transmission but the reciprocal position vary quite rapidly, as the satellite rotates around the north pole. The use of a highly directional antenna, with a narrow beam, would increase the amount of power spread into its main direction but, on the other end, it would need to be constantly re-orientated towards the receiver in order to grant a long contact period. The use of moving mechanical components would increase the complexity of the system and the probability of failure. For an omni-directional antenna, instead, the power is equally spread into every direction and the amount of power that reaches the ground station is lower than the prior case, as it decreases proportionally to the square of the distance. However, it permits to communicate easily during all the visibility period without the necessity of redirection. An omni-directional coverage was chosen for the S-band link: TM and TC do not have a large amount of data volume and for this reason a high directivity, and a higher power, it's not necessary; furthermore an omni-directional antenna allows the satellite to communicate with the ground station even if it's disoriented, and to re-align itself. For the science data, however, a much higher volume need to be transmitted in the same amount of time and a higher directivity of the antenna is then required. The selected antenna consists of a combination of two coaxial radiators, namely a two-hybrid-mode horn and a bi-conical antenna. The bi-cone is designed to provide the main beam peaks at the edge of the coverage area ( $\theta = 62^\circ$ ), a fast drop (high slope) outside the coverage area, and a low back-radiation. On the other hand, the horn fulfils the pattern in the boresight ( $\theta = 0^\circ$ ) and near-in angular region ( $|\theta| < 40^\circ$ ). In this way a higher directivity than an omni-directional antenna is granted but still the beam it's not so narrow to require a re-direction towards the receiver.

In addition to the links described previously, MetOp provides also an Advanced DCS (Argos) service and a Search & Rescue (SARR/SARP) service. These services need to guarantee communication with a range as wide as possible; for this reason omni-directional antennas were picked also in this case. The total amount of antennas implemented on the MetOp-A satellite are then eight. To resume:

- X-band transmit antenna (coaxial bi-cone/horn RHCP circularly polarized antenna)
- S-band TT&C receive antenna (omni-directional RHCP circularly polarized antenna)
- S-band TT&C transmit antenna (omni-directional RHCP circularly polarized antenna)
- LRPT VHF transmit antenna (omni-directional RHCP circularly polarized antenna)
- HRPT L-band transmit antenna (omni-directional RHCP circularly polarized antenna)
- CRA: Combined Receive Antenna (up-link) (omni-directional linearly polarized antenna)
- SLA: Search and Rescue L-band transmit antenna (omni-directional linearly polarized antenna)
- DTA: DCS transmit antenna (omni-directional RHCP circularly polarized antenna)

### 3.3.5 Link budget

In order to compute the link budget of the satellite, knowing the kind of hardware that is on-board, the first step to do is to convert all data into decibels and compute the parameters of the antennas. Since the evaluation of the link budget follows the same steps for each link, it has been analyzed for the X-band; the same formulas can be applied also to the other links.

At first the fundamentals parameter of the ground station antenna are computed, them being the gain and the beam-width. In order to calculate the gain of the antennas of the CDA, we need to know the diameter of the dishes. The station has grown continuously since 1996 and consist today of six large antenna installations operating in L-, S-, and X-band. The antennas have between 9 and 13 m diameter dishes and are equipped with necessary back-end and monitoring equipment. The Global Data Stream down-link operate in X-band with a frequency domain of 7750-7900 MHz; from this frequency it can be deduced the respective wavelength:  $\lambda = \frac{c}{f}$  ( $\lambda_{rx} = 0.038$  m). The antenna gain is then computed with the formula:

$$G_{rx} = 10 \log \left( \frac{\pi D_{rx}^2 \mu_{rx}}{\lambda_{rx}^2} \right) \quad (3.3)$$

where  $\mu$  is antenna's efficiency given by the shape; parabolic antennas have  $\mu = 0.55$ . The result considering a diameter of 10 m is a gain of approximately 50 dB. The beam-width is computed by the formula:

$$\theta_{rx} = \frac{65.3 \lambda_{rx}}{D_{rx}} \quad (3.4)$$

The result, still considering a diameter of 10 m, is  $0.24^\circ$ .

The parameters of the transmitting antenna are instead obtained from the literature: for this particular coaxial bi-cone/horn antenna the gain at a frequency of around 7.8 GHz, as in our case, is roughly 6 dB.

As already said the formulas for the S-Band up-link are the same: with a domain of 2053.4 MHz the wavelength results 0.146 m. Omnidirectional antennas on satellites have typical diameters between 10-30 cm. So  $G_{rx}$  is approximately 6.2 dB.

After the definition of these parameters an analysis of the losses has been done.

**Cable Losses** The losses due to the use of cables are typically between -1 dB and -3 dB; as this is only a preliminary design, they'll be assumed at 3dB for the worst case scenario.

**Free Space Losses** The Space Losses depends on the distance between the satellite and Ground Station and on the carrier frequency by the formula:

$$L_{space} = 20 \log \left( \frac{\lambda}{4\pi r} \right) [dB] \quad (3.5)$$

The wavelengths, computed previously, are 0.038 m and 0.146 m. The distance has been approximated to roughly 1000 km. The result is then a loss of 170.4 dB for X-Band and a loss of 158,7 for S-Band.

**Pointing Losses** The losses due to the pointing of the antenna depends on the pointing accuracy and receiver beam-width by the following formula:

$$L_{pointing} = -12 \left( \frac{\eta}{\theta_{rx}} \right)^2 [dB] \quad (3.6)$$

where  $\eta$  is the parameter representing pointing accuracy and it is roughly 0.1. The result is a loss of 2.08 dB. No pointing losses for the omnidirectional-antenna.



**Atmospheric Losses** The power loss due to the interference of the atmosphere and the rain attenuation was obtained from the literature: 0.05 dB.

Knowing all the losses and the antennas parameters is then possible to determine the EIRP (Effective Isotropic Radiated Power) and the total Receiver Power. The EIRP is computed next as:

$$EIRP = P_{tx} + G_{tx} + L_{cable}[dB] \quad (3.7)$$

As no complete data were available on the overall transmitting power, it was fixed a value of 100 W for the X-band transmission and a value of 40 W for the S-band transmission. These values were deduct as reasonable transmission power from the literature. Also from the literature was derived the gain of the X-band antenna: as already mentioned above, the gain of a coaxial bi-cone/horn antenna is approximately 6 dB. The gain of the transmitting antenna for the up-link is instead the gain of the ground station antenna. On this assumption, the resulting EIRP is of 23 dB. The receiver power is computed as:

$$P_{rx} = EIRP + G_{rx} + L_{space} + L_{atmosphere} + L_{point}[dB] \quad (3.8)$$

It result to be -99.52 for X-Band and -129.7 for S-Band.

Noise density can be computed using an average temperature of the GS as:

$$N_0 = 10\log(kT_s) \quad (3.9)$$

where k is the Boltzmann constant equal to  $1.38 \times 10^{-23}$  Js/K and the sensor temperature can be approximated around 290 K. The result is a noise density around -204 dB.

Knowing the received power, the noise density and data-rate, it is possible to compute the Error per bit to Noise density as:

$$\frac{E_b}{N_0} = P_{rx} - N_0 - 10\log(R_{real}) \quad (3.10)$$

which result as 26.03 dB for the X-Band down-link and 41.39 dB for the S-Band up-link.

Considering that the desired BER (bit error rate) has typical values that range from  $10^{-5}$  for TM and data down-link and  $10^{-7}$  for TC up-link, and therefore the consequent  $E_b/N_0$  minimum to achieve for a RS encod is around 5.5 dB, it is possible to say that there is a good margin and the receiver has the capability to translate the signal, distinguishing it from the noise.

The modulation index  $\beta_{mod}$  depends on the receiver, usually is between  $45^\circ$  -  $90^\circ$ . In this case it has been considered  $\beta_{mod} = 78^\circ$  as no informations were given a priori.

The power removed from the carrier due to modulation is the Carrier Modulation Index Reduction, calculated as:

$$P_{mod,loss} = 20\log(\cos(\beta_{mod}))[dB] \quad (3.11)$$

that results equal to -13.64 dB.

Therefore the Carrier Power is computed as:

$$P_{carrier} = P_{rx} + P_{mod,loss}[dB] \quad (3.12)$$

so -113.16 dB for X-Band and -140.34 dB for S-Band

In the end, knowing the receiver bandwidth B, that is usually around 30 Hz, it is possible to compute signal-to-noise ratio:

$$SNR_{carrier} = P_{carrier} - N_0 - 10\log(B) \quad (3.13)$$

so 75.89 for X-Band and 48.89 dB for S-Band.

For a typical LEO satellite telemetry communication system, a common target SNR to achieve a reasonable BER is around 10 to 15 dB, depending on the specific requirements of the mission and the system design choices such as the ground station characteristics. It has been therefore assumed  $SNR_{minimum} = 10dB$  and the margin can be computed:

$$SNR_{margin} = SNR_{carrier} - SNR_{minimum} \quad (3.14)$$

with a 65.89 for the X-Band and a 38.89 for the S-Band.

## Chapter 4

# Attitude and Orbit Control Subsystem

Change Log	
4.1 Control modes	Pages 24-25: Requirements of different control modes better explained.
4.3 Actuators selection	Page 26: Reaction wheels input parameters corrected; Reaction wheel functioning explained better; Figure 4.2: added short image description.
4.4.2 Disturbances effects	Page 27: Gravity gradient torque and magnetic torque values approximated with less decimal digits.
4.4.3 Attitude sensors sizing and pointing budget	Page 28: Table 4.1 revised.
4.4.4 Attitude actuators sizing	Page 28: Added Figure 4.3.
4.4.4 Attitude actuators sizing	Page 29: Added "Reaction Wheels sizing" subsection.

Attitude and Orbit Control Subsystem (AOCS) is responsible for attitude determination, orbit maintenance and Earth pointing with sufficient precision to grant good working conditions for all the instruments onboard the satellite. It includes all the hardware (attitude sensors and actuators), software (orbit control algorithms) and a navigation system (GPS) to perform satellite's attitude determination and orbit control as required by the mission drivers.

AOCS shall provide the orientation of the spacecraft during all different phases of the mission, and it shall also guarantee, in case of major anomaly, that safe mode start operating autonomously to ensure satellite's integrity and avoid damages to the instrumentations.

Different phases of MetOp mission require different accuracies both in orbit determination and control, that means different levels of precision in the set of sensors and actuators installed on the spacecraft.

Another thing to consider, is the presence of some disturbing effects that deviate our real orbit from the ideal, unperturbed one. These disturbance torques, in the case of a satellite orbiting in LEOP like MetOp does, are mainly due to air drag, solar radiation pressure, Earth's gravitational and magnetic fields.

### 4.1 Control modes

In the following section are presented the four principal control modes of MetOp-A's AOCS. The satellite requires a very precise design of attitude subsystem to satisfy each of the main control modes of the mission.

**Operative mode:** As all the instruments have very high accuracy and sensitivity, to work in nominal conditions they need that the spacecraft will maintain a very stable and accurate relative attitude with respect to the Earth during all data acquisition phase.

For this reason, MetOp satellite is three-axis stabilised, and the attitude control is granted by the reaction wheels, that are a good choice for fine and very precise manoeuvres for satellite stabilisation. These actuators need to be desaturated at some point, and for this reason onboard the spacecraft are mounted a couple of magneto-torquers as well.

**Communication mode:** MetOp-A is orbiting on a low Earth polar orbit with a period of about 101 minutes. Every orbit it passes over ground station and it has a visibility of 12 minutes in which all data collected from the instruments are sent down to the Earth by all the antennas discussed in the TTMTTC subsystem. In addition to that, on-ground Mission Control System (MCS) and Flight Dynamics Facility (FDF) control the satellite through a set of commands (AOCS TCH) sent twice per day.

During this phase, spacecraft's antennas must point towards the Earth in order to ensure proper communication for all the visibility window, and therefore MetOp AOCS shall provide and maintain the correct relative position between the satellite and Earth. In this control mode the level of performance needed is not so strict like the one of operative mode, but high accuracy is still required. Therefore, in this operational mode satellite's attitude is controlled by reaction wheels and magneto-torquers.

**Orbit control mode:** The orbit maintenance of MetOp-A satellite consists of three types of manoeuvres:

- Short in-plane (SIP) manoeuvres, with a burn duration of less than 30 seconds at the beginning of mission (1 minute at EOL);
- Long in-plane (LIP) manoeuvres;
- Out-of-plane (OOP) manoeuvres;

SIP manoeuvres are performed in yaw-steering attitude pointing mode (YSM), whereas LIP and OOP manoeuvres are in fine pointing attitude mode (FPM), that grants a more precise control law, and consequently higher accuracy in performance error. All these three types of manoeuvres are performed by thrusters, used in different combinations. For IP manoeuvres, the onboard AOCS activates a series of small thruster pulses to correct for the attitude pointing after the main burn. These pulses typically last for approximately 2-6 minutes and their impact cannot be neglected for short IP maneuvers.

**Slew manoeuvre:** OOP manoeuvre comprises five thrusting phases: start slew, stop slew, main burn, start anti-slew and stop anti-slew. [Figure 4.1]

The execution of OOP manoeuvres is restricted to periods when the spacecraft is in eclipse. This is to protect the scientific instruments from exposure to the Sun when the spacecraft is performing the slew and anti-slew manoeuvres. Prior to the slew manoeuvre, the spacecraft changes its attitude guidance law from YSM to FPM. Thereafter, the spacecraft is slewed to align the propulsion thrusters in the direction normal to the flight direction. Upon completion of the OOP thrust phase, the anti-slew maneuvers are commanded to return to the nominal flight configuration. In the end, the satellite changes again its attitude control law, from FPM to YSM, though this transition can occur even half an orbit later than the end of the manoeuvre. The switching of attitude guidance law is performed to prevent the possibility of introducing errors in the velocity vector

that result in wrong, undesired manoeuvres. Errors are due to thrusters unbalance, uncertainties in thrust level, on/off transients. So, a very accurate control mode ensures the minimum effects of these errors on satellite's operational life.

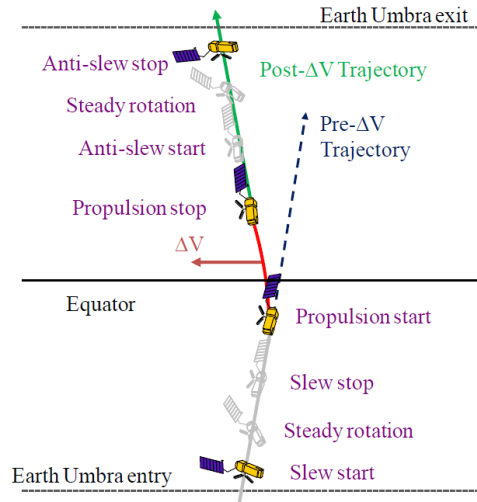


Figure 4.1: *MetOp-A's out-of-plane manoeuvre sequence*

**Safe mode:** The design of the Service Module (SVM) ensures 36 hours of autonomy on board during which the mission performance requirements will be maintained. There is extensive on-board monitoring with automatic re-configuring in case of an anomaly. In most cases of SVM anomaly, this results in load-shedding and the Payload Module (PLM) is switched off. In case of severe or double failure, there is a safe mode (SFM) which is a very stable sun-pointing mode under the control of a separate processor that can ensure safety conditions to the satellite up to 7 days.

## 4.2 Sensors selection

The AOCS uses the Sun sensor for yaw control, the Earth sensor for pitch and roll control, and four bi-axial gyros (two being in redundancy). During the LIP and OOP maneuvers, the spacecraft attitude is automatically controlled using the attitude and coupled thrusters as commanded by the AOCS. This attitude mode is equivalent to the nominal attitude pointing or geocentric pointing. As for the SIP maneuver, the AOCS automatically activates the attitude thrusters to correct the yaw-steering attitude pointing after the main burn terminates. These attitude corrective/stabilization thrust pulses can last up to 6 minutes. Attitude stabilization also applies to LIP maneuvers. It occurs after the main burn to re-establish the FPM before transitioning back to YSM guidance.

## 4.3 Actuators selection

MetOp-A has on board different types of actuators that are used in different situations. There are the set of eight mono-propellant, hydrazine-based thrusters mentioned in PS subsystem, plus another set for redundancy. All the engines are mounted in pairs, and depending on the face of the spacecraft on which are installed, they can provide only a torque effect (attitude control thrusters) or both torque and thrust (coupled thrusters). Thrusters are used for slew/anti-slew, large in-plane and out-of-plane manoeuvres.

Besides them, there are also three reaction wheels (RWs), each of them has a momentum storage capacity of 40 Nms and provides a maximum net torque capability of 0.2 Nm. Three RWs are sufficient to grant very precise three-axis attitude control. These actuators work during operative and communication modes, to keep spacecraft's position fixed in space.

As angular rate grows, the torque level provided by the wheels remains almost constant across the full speed range. But when the maximum operational speed is reached, torque will rapidly drop to zero: this is the so-called saturation phenomenon.

After reaching this condition, RWs need a special desaturation mechanism to make them operational again, and for MetOp it has been decided to install two magneto-torquers able to generate a  $315 \text{ Am}^2$  magnetic moment. In Figure 4.2 it is shown an approximation of the characteristic curve of a generic reaction wheel. This is a qualitative graph, just to show how is the torque-speed curve of a reaction wheel. Axes are not gridded because these actuators have a wide range of torque level, based on the size of the satellite on which they are mounted on. Typically, reaction wheels are capable of generating torque that ranges from a few mNm, to 200-250 mNm and keep this torque level almost constant for all the nominal speed range, up to 4000-6000 rpm. Above that speed, torque will drop to zero rapidly.

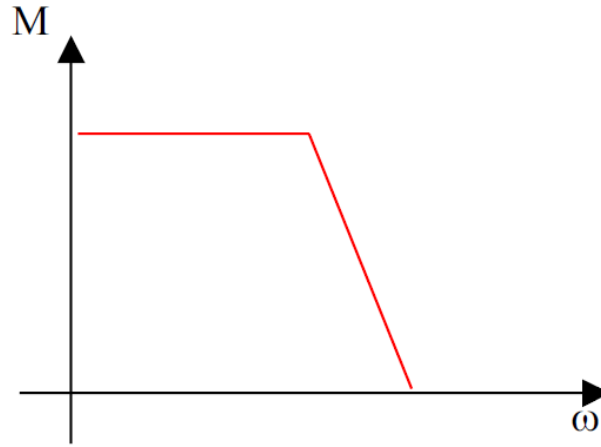


Figure 4.2: *Speed ( $\omega$ ) vs. Torque ( $M$ ) for a generic reaction wheel.*

## 4.4 Reverse sizing

### 4.4.1 Satellite dimensions and Inertia matrix

The overall size reported for the MetOp-A satellite in the on-orbit configuration is  $17.6 \times 6.7 \times 5.4 \text{ m}$ . In order to calculate the inertia matrix the main body of the spacecraft is geometrically assumed to be shaped like a rectangle block with size of  $6.5 \times 3.5 \times 3.5 \text{ m}$ , and the solar panel assumed as a flat plate measuring  $7 \times 6.7 \text{ m}$ .

The inertia matrices of these two elements have been computed separately, considering two reference systems, one for the solar panel ( $\text{RF}_{SA}$ ), the other for the main body ( $\text{RF}_B$ ). Then, thanks to Huygens-Steiner theorem, matrix relative to solar array has been evaluated again, with respect to  $\text{RF}_B$  this time, so that it can be easily added to the one of spacecraft body to find inertia matrix of the whole satellite. The resulting matrix is:

$$\begin{bmatrix} 21268 & 0 & 0 \\ 0 & 21298 & 0 \\ 0 & 0 & 28499 \end{bmatrix} \text{ kg} \cdot \text{m}^2$$

### 4.4.2 Disturbances effects

Disturbances sources in attitude are gravity gradient, solar radiation pressure, aerodynamic drag and magnetic field of the orbiting planet.

**Gravity gradient torque** is:

$$T_{gg} = \frac{3\mu}{2R^3}(I_{max} - I_{min})\sin(2\theta) \quad (4.1)$$

The angle  $\theta$  is the maximum deviation of the z-axis from the local vertical (in radians), and in this case it will be assumed be  $\frac{\pi}{4}$  in order to have the highest possible disturbance and analyze the worst case scenario,  $\mu$  is Earth's gravitational constant and  $R$  is the distance of the satellite from the center of the Earth. **The resulting torque is nearly 0.02 Nm.**

**Solar Radiation Pressure (SRP)** can be computed with the following equation:

$$T_{SRP} = \frac{F_s}{c}A_s(1 + q)\cos(I)(c_s - c_g) \quad (4.2)$$

However this disturbance can be neglected, due to the fact that the mission is operated below 1000 km of altitude (12).

**Aerodynamic drag**, as SRP perturbation, at the altitude where is orbiting MetOp-A has a negligible value with respect to the disturbance torque due to gravity gradient. That is because the air density at a mean orbit altitude of 824 km, computed using *CIRA-72* Atmospheric model [Equation 4.4], has a value of  $\rho = 9.65 \cdot 10^{-15} \frac{kg}{m^3}$ .

$$T_{drag} = \frac{1}{2}\rho C_d A v^2 (c_{ap} - c_g) \quad (4.3)$$

$$\rho = \rho_0 e^{-\frac{h-h_0}{H}} \quad (4.4)$$

And, assuming the worst-case scenario where the distance between aerodynamic and gravity centers is the maximum possible, 17.6 m, it gives as a result a disturbance torque of  $7.204 \cdot 10^{-10}$  Nm, confirming the initial assumption.

**Magnetic torque** is:

$$T_{mag} = DB \quad (4.5)$$

The precise value of  $D$  has to be obtained with tests on the residual dipole. However, by knowing that  $D$  depends on the mass and supposing that ESA missions have very high quality standards, it can be done a rough estimation based on a literature survey (13) that gives as a result a value of  $4.1 \text{ Am}^2$ . The resulting torque is  **$2 \cdot 10^{-4} \text{ Nm}$ .**

### 4.4.3 Attitude sensors sizing and pointing budget

In the following table sensors of MetOp-A are listed, with their typical values of mass and power. The number of gyroscopes includes the redundant ones. The horizon sensor is assumed to be fixed due to the fact that is the most used type for LEO orbiting satellites. A column with the typical values of accuracy gives the pointing budget

Sensor	Number	Mass [kg]	Power [W]	Typical performance range
Gyroscope	4	0.1 to 15	1 to 200	0.003 deg/hr to 1 deg/hr
Sun Sensor	2	0.1 to 2	0 to 3	0.005 deg to 3 deg
Horizon Sensor	2	0.5 to 3.5	0.3 to 5	0.1 deg to 0.25 deg

Table 4.1: *List of MetOp-A attitude sensors.*

#### 4.4.4 Attitude actuators sizing

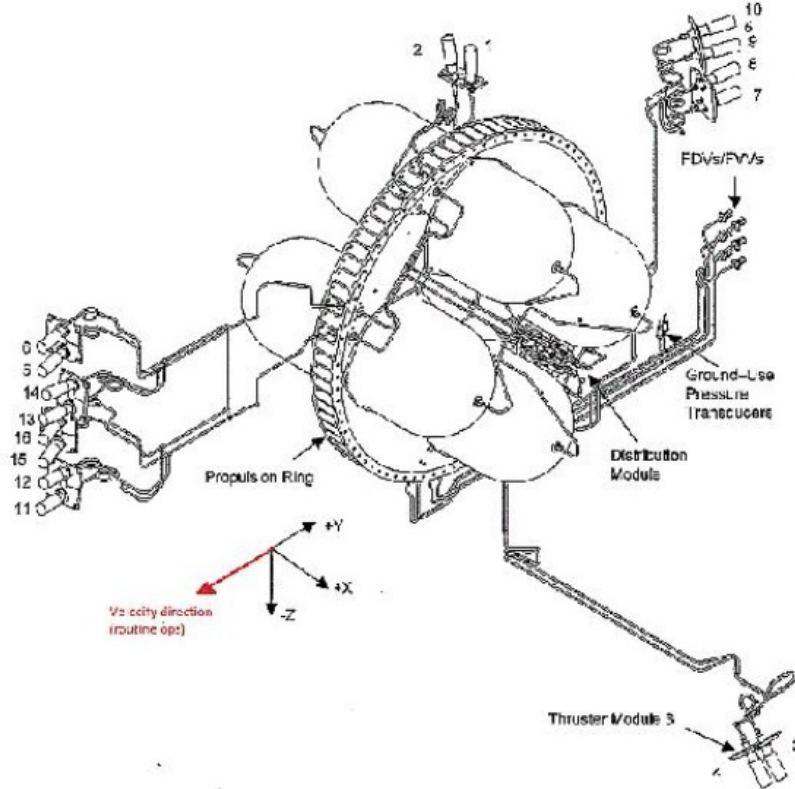
##### Thrusters sizing

Actuators have to be sized in order to compensate effects of disturbances and to perform the needed slew maneuver to have the desired attitude.

The required force needed to compensate disturbances is:

$$F_{th} = \frac{T_d}{nL} \quad (4.6)$$

$T_d$  is the total disturbance torque affecting the spacecraft. By adding all values computed it is obtained a value of **0.02 Nm**.  $n$  and  $L$  represent the number of the thrusters and arm. Usually torque disturbance compensation is not the sizing manoeuvre, because the force needed is very small. This can be confirmed by computing with 8 thrusters, which is the number onboard of MetOp, and an average arm of 6m, **assumed to be this one because of the section of the spacecraft in the plane that contains all the thrusters, which is 6.7m x 5.4m**. The value of the **section matches the scheme of the thrusters positioning that can be seen in Figure 4.3**. The result is  $2.45 \cdot 10^{-4}$  N.

Figure 4.3: *Thrusters positioning in MetOp-A*



The force needed for slew manoeuvre is:

$$F_{th} = \frac{I_{sc}\ddot{\theta}}{nL} \quad (4.7)$$

while the acceleration rate is:

$$\ddot{\theta} = \frac{\theta}{t_{slew}t_{slew,acc}} \quad (4.8)$$

A literature survey (12), based on the data of the EUMETSAT out of plane maneuvers performed in 2008 and 2009, gives an average  $\theta$  of  $88.14^\circ$  and slew time 360s. The angles considered for the estimation are the commanded rotations of the spacecraft (Table 5 of (12)), whereas the slew time it's estimated by the report (Table 9 of (12)). For the spacecraft inertia it will be considered the highest one on the inertia matrix, in order to consider the most requiring scenario. By remembering that the slew acceleration time is half the total slew time is possible to compute a thrust force of 0.8 N. The thrusters system is fueled by 316 kg of hydrazine (15).

### Reaction Wheels sizing

Reaction wheels are essential components of many spacecraft and have proven to be efficient, reliable, and versatile for precise attitude control and stabilization. The reaction wheels in MetOp-A specifically are used in order to counteract the torque disturbances that occur when the spacecraft is in orbit. The total torque that the reaction wheels need to counteract can be calculated by considering a 250% safety margin on the total disturbance torque:

$$T_{RW} = \eta T_D \quad (4.9)$$

The resultant torque is 0.05 Nm. The momentum storage of the reaction wheels can be computed as it follows:

$$h_{RW} = T_D \frac{t_{orbit}}{4} 0.707 \quad (4.10)$$

By considering an orbital period of 101.4 minutes the resulting momentum storage is 21.5 Nms. The results are acceptable if compared with the data sheet of a typical reaction wheel on board of ESA spacecrafts (18).

## Chapter 5

# Thermal Control Subsystem

The Thermal Control System (TCS) consists of the hardware in charge of keeping each component on the spacecraft in its optimal working temperature range.

There are several issues that have to be taken into account when designing a TCS and they are strictly dependant on the mission. For instance, a deep space mission will more likely not have to worry about the albedo of a planet as much as a mission orbiting that planet.

When designing a TCS both cold and hot case have to be defined as both cooling needs and strategies might differ from an eclipse phase and an exposed one. The first one might require heaters while the latter radiators or heat exchangers. For a satellite the main heat exchange modes that will be considered are conduction and radiation as convection is in general limited to habitat and atmospheric phases.

It is important to have a thorough understanding of optical properties such as reflectance  $\rho$ , absorptance  $\alpha$ , transmittance  $\tau$  and emittance  $\epsilon$ . As the radiative heat exchange is strongly influenced by the view factor, the layout of the satellite is also important and should be carefully analyzed. Among the heat sources are: Solar flux, albedo, IR and BETA angle. These heat sources affect the power generate on board, that has to be entirely dissipated towards outer space through radiation.

A preliminary analysis will be performed assuming steady state conditions and modeling the spacecraft as a sphere (single nodal approach).

When designing the spacecraft it is good norm to adopt safety margins on the temperatures reached. The more advanced the design phase the smaller the margins should be.

Thermal control solutions can be active or passive. Usually the first ones grant a higher performance at the cost of a greater complexity. In general, for both solutions degradation should be considered as the space environment is particularly tough on the components. In order to provide adequate performance at EOL, a slight over design will be necessary.

## 5.1 TCS solution identification, rationale, justification

The MetOp-A satellite was designed considering the spacecraft made out of two different block: Payload module (PLM) and service module (SVM). Different cooling strategies were investigated for both blocks.

### 5.1.1 PLM TCS

Thermal control of the PLM is passive (i.e. radiators and MLI) and supplemented by heaters. These are the main elements of the thermal control: a Multi-Layer-Insulation (MLI), flexible second surface mirror radiators, thermal doublers to spread the heat of high dissipating units, a black paint on inner side of PLM panels, hardware controlled heaters as well as software con-

trolled heaters and monitoring thermistors. Most instruments have their own thermal control and are thermally de-coupled from the PLM structure.

### 5.1.2 SVM TCS

Four main areas of the Service Module need thermal control:

- The main body, where all the heat dissipating units are installed on the side and floor panels. The external radiators are finished with silvered FEP Teflon tape. Multi-Layer-Insulation (MLI) blankets cover all the other faces of the main body to minimise the heat flow. Internally the panel and the electronics units are black painted to maximise the radiative exchanges.
- The batteries, directly mounted on a radiator plate and enclosed in a compartment, which is thermally insulated from the rest of the spacecraft.
- The propulsion equipment, conductively insulated from the spacecraft; the tanks and piping are temperature controlled using MLI and heaters.
- The solar array, which once deployed, provides its own thermal control (using passive means such as MLI and adequate thermal finishes). Active thermal control (heaters) is used only during the period after the separation of the spacecraft from the launcher and up to the completion of the solar array deployment.

### 5.1.3 Thermal heat sources during the mission

The external and internal thermal fluxes encountered by the spacecraft remain almost unvaried during the different phases of the mission from a global point of view. Since the satellite is designed for a meteorological mission around the Earth, the heat sources and the heat sinks with whom it has to deal stay the same.

The possible heat sources are the Sun, the internal power, the Earth Albedo and the Earth IR; among these, the internal power and the Earth IR are always present, while the heat due to the Sun and to the Earth Albedo is not present when the satellite find himself in a condition of eclipse.

The primary heat sink is always just the deep space.

What does change through the different phases is the amount of internal heat produced; that's because during the initial phases of verification and calibration of the performances of the satellite, namely LEOP and SIOV, the instrumentation was not yet operative.

### 5.1.4 Temperature intervals

The temperature requirements of the instruments and equipment on board are the main factors in the design of the thermal control system. Keeping all the components in their optimal operational temperature range is crucial for every mission. Some examples of temperature ranges include:

- Batteries have a very narrow operating range, typically between  $-5^{\circ}\text{C}$  and  $20^{\circ}\text{C}$ .
- Internal propulsion components have a typical range of  $5^{\circ}\text{C}$  to  $40^{\circ}\text{C}$  for safety reasons.
- For ACS and for C&DH Electronics is between  $-20^{\circ}\text{C}$  to  $50^{\circ}\text{C}$ .
- For actuators and Flexible Harness is between  $-55^{\circ}\text{C}$  to  $50^{\circ}\text{C}$ .

- For antennas is typically between  $-100^{\circ}\text{C}$  to  $40^{\circ}\text{C}$ .
- Solar arrays have a wide operating range of  $-150^{\circ}\text{C}$  to  $100^{\circ}\text{C}$ .
- Propulsion System has a typical range of  $-20^{\circ}\text{C}$  to  $40^{\circ}\text{C}$ , but hydrazine has a lower allowable limit of  $10^{\circ}\text{C}$ , since it freezes at  $2^{\circ}\text{C}$ ; hence propellant tanks and lines have a range between  $10^{\circ}\text{C}$  and  $40^{\circ}\text{C}$ .

Considering the more stringent requirements, the temperature must be kept between  $10^{\circ}$  and  $20^{\circ}$ ; however, since the gradient temperature admissible across optical instruments needs to be lower than  $5^{\circ}\text{C}$  and since a mean temperature  $10^{\circ}\text{C}$  greater can reduce by a factor 2 the life duration of electronic components, it has been decided to fix a temperature interval of  $10^{\circ}\text{C}$ - $15^{\circ}\text{C}$ , assuring a more conservative analysis.

## 5.2 Reverse engineering

### 5.2.1 Thermal fluxes

As already said, there are four thermal heat sources that act on the spacecraft: the Sun, the internal power, the Earth Albedo and the Earth infrared radiation. Each one of these comport a different thermal flux.

**Solar flux** The solar flux it's easily calculated, as it only depends on the distance between the Sun and the spacecraft trough the formula:

$$q_{sun-sc} = q_0 \left( \frac{R_{Earth}}{R_{sc}} \right)^2 \quad (5.1)$$

where  $R_{sc}$  is the distance of the spacecraft to the Sun.

Since in this case the satellite is in orbit around the Earth, it can just be consider the solar flux equal to  $q_0$ , which is  $1367.5 \text{ W/m}^2$ .

**Albedo flux** The Albedo flux depends on the fraction of incident sunlight reflected by the planet. Considering that the planet radiate uniformly from the whole cross-sectional area, it can be evaluated with respect to the orbital height with the following formula:

$$q_{albedo,pl} = q_{sun-sc} a \cos(\theta) \left( \frac{R_{pl}}{R_{orbit}} \right)^2 \quad (5.2)$$

where  $R_{pl}$  is the planet radius, which for the Earth is 6371 km, while  $R_{orbit}$  is the spacecraft orbital radius, given by the sum of the planet radius and the orbital height; in this case the orbit is near-circular with a mean altitude of 817 km therefore the  $R_{orbit}$  result to be 7188 km. The parameter  $a$  is instead the albedo factor, which for the Earth it's around 0.35. Finally  $\theta$  represent the irradiance angle between the spacecraft and the planet; in order to be more conservative it has been considered the worst case scenario, in which the irradiance is perpendicular to the surface of the spacecraft and the cosine of  $\theta$  is 1. Having defined all the parameters of the equation it is possible to calculate the albedo flux, which result approximately  $376 \text{ W/m}^2$ .

**Infrared flux** The infrared flux depends on the surface temperature of the planet or space bodies around which the spacecraft is orbiting, that in this case it's only the Earth. It can be calculated with the formula:

$$q_{IR,pl} = \sigma \epsilon T_{pl}^4 \left( \frac{R_{pl}}{R_{orbit}} \right)^2 \quad (5.3)$$

where  $\sigma$  is the Stefan-Boltzmann constant ( $5.67 \times 10^{-8} \text{ W/m}^2\text{K}^4$ ),  $\epsilon$  is the infrared emissivity of the planet (0.98) and  $T_{pl}$  is the surface temperature of the planet (288.15 K). The infrared flux due to the Earth is then roughly  $300 \text{ W/m}^2$ .

### 5.2.2 Hot and cold case identification

As previously anticipated, the worst cold condition happens during the eclipse, when both Sun and Albedo flux are absent, and when the internal power is minimum, that being in this case when the instrumentation is off.

The worst hot condition, instead, is when the spacecraft is hit by all the possible fluxes and when the internal power consumption is at maximum, with all the instruments fully operative.

In order to determine the internal generation of heat for the two separate cases, it is necessary to evaluate the efficiency of the power transmission. This efficiency can be at first calculated as the ratio between the generated power and the actual power consumption:

$$\eta = \frac{P_{out}}{P_{in}} \quad (5.4)$$

It's however important to point out that it constitute an approximation because in this way it's not taken into account a possible redundancy of power.

The average power derived from the solar panel over one orbit is approximately 2210 W (EOL condition), while the total power consumption is around 1810 W. Therefore the estimated efficiency is roughly 0.819.

At this point it's possible to obtain the internal heat flux as:

$$Q_{int} = (1 - \eta)P_{in} \quad (5.5)$$

which result to be 400 W.

This evaluation was done with the total consumption of the satellite, including the instruments power consumption, therefore the result represent the hot case internal power generation. To determine the cold case it has been considered the same efficiency of power transmission, since the overall system doesn't change, and it has been done a proportion between the total power consumption and the partial consumption of just SVM and PLM.

The internal power for the cold case results to be roughly 205 W. In conclusion:

$$Q_{int,max} = 400W \quad (5.6)$$

$$Q_{int,min} = 205W \quad (5.7)$$

Steady state conditions can be used as preliminary analysis, modelling the spacecraft as a point mass. For both hot and cold cases the sum of the total input heat, the total internal heat and the total output heat must be zero:

#### Hot Case

$$Q_{sun-sc} + Q_{albedo,pl} + Q_{IR,pl} + Q_{int,max} - Q_{emitted} = 0 \quad (5.8)$$

#### Cold Case

$$Q_{IR,pl} + Q_{int,min} - Q_{emitted} = 0 \quad (5.9)$$

### 5.2.3 Heat powers

The others heat powers depend on the external and internal thermal heat sources and flux defined previously. They can be calculated modelling the spacecraft through a single-node equivalent sphere. In the first place it is possible to defined a total area of this equivalent sphere starting from the lateral dimension of the spacecraft:

$$A = 2(l_1l_2 + l_2l_3 + l_1l_3) \quad (5.10)$$

After that, the radius of the sphere can easily be determined:

$$r_{sp} = \sqrt{\frac{A}{4\pi}} \quad (5.11)$$

For MetOp-A the lateral dimension are 6.2 m, 3.4 m and 3.4 m (without considering the solar panel). Therefore the equivalent spherical area is around 107,44 m<sup>2</sup> and the radius is 2.924 m.

**Emitted Power** The spacecraft exchange with the external deep-space an amount of power equal to (for an equivalent sphere):

$$Q_{emitted} = \sigma \epsilon A (T_{sc}^4 - T_{space}^4) \quad (5.12)$$

where  $A$  is the fraction of spacecraft area that radiates, while  $\epsilon$  is the spacecraft emissivity. The latter is determined by the used coating strategy; considering at first just a general polished metal, it is around 0.15.

#### Solar Power

$$Q_{sun-sc} = A_{cross} \alpha q_{sun-sc} \quad (5.13)$$

where  $A_{cross}$  is the fraction of spacecraft exposed area with respect to the sun (cross sectional area), computed by the formula  $A_{cross} = \pi r_{sc}^2$ , which in this case is roughly 26.86 m<sup>2</sup>.

Like the emissivity also  $\alpha$ , which is the spacecraft solar absorptivity, is defined by the coating and for a polished metal is 0.2.

The solar power is in this case 7346.21 W.

#### Albedo Power

$$Q_{albedo,pl} = A F_{pl-sc} \alpha K_a q_{albedo,pl} \quad (5.14)$$

$A$  is the single-node area, already defined;  $K_a$  is the diffusion factor of the planet, and since it's value vary between 0 and 1 it has been considered the worst case scenario, taking  $K_a = 1$ ; lastly,  $F_{pl-sc}$  is the planet-spacecraft view factor, computed by the formula:

$$F_{pl-sc} = \frac{1}{2} \left( 1 - \frac{\sqrt{\left(\frac{h}{R_{pl}}\right)^2 + 2\frac{h}{R_{pl}}}}{1 + \frac{h}{R_{pl}}} \right) \quad (5.15)$$

where  $h$  is the orbital height (817 km).

The view factor result to be 0.268 and, at this point, the albedo power can be determined: 2165.3 W.

#### Infrared Power

$$Q_{IR} = A F_{pl-sc} q_{IR,pl} \quad (5.16)$$

Having already defined all the parameters of the equation, the infrared power is calculated: 8638.17 W.

### 5.2.4 Control strategy

**Hot case computation** Considering the hot case scenario, in the heat power balance defined previously the only unknown is the spacecraft temperature:

$$T_{sc} = \sqrt[4]{\frac{Q_{int,max} + Q_{sun-sc} + Q_{albedo,pl} + Q_{IR,pl}}{\sigma \epsilon A}} \quad (5.17)$$

This temperature, 377.46 K, is definitely outside the range required, hence a passive or active cooler must be introduced. It has been analyzed the possibility of a cooling system with radiators; radiators, that have a high emissivity, can be of two types: deployables, increasing the spacecraft surface, or panels positioned directly on the spacecraft surface. The second type has been considered at first, as it doesn't change the satellite dimension. In this case it is possible to compute the minimum radiators surface through the formula:

$$A_{rad,min} = \frac{Q_{int,max} + Q_{sun-sc} + Q_{albedo,pl} + Q_{IR,pl} - \sigma \epsilon_{sc} A T_{max}^4}{\sigma (\epsilon_{rad} - \epsilon_{sc}) T_{max}^4} \quad (5.18)$$

The necessary radiators area for this case result to be approximately 42.93 m<sup>2</sup>, which is quite high. It has been therefore considered the application of a better coating: Aluminized Kapton. For an aluminized kapton coating with a thickness of 0.5 mm the emissivity is 0.55 and the absorptivity is 0.4.

The hot case temperature result 302,51 K and therefore the necessary radiators area is 38.4 m<sup>2</sup>.

Increasing the thickness of the insulation layer it is possible to reduce even more the radiators area; this could however worsen the cold case scenario.

**Cold case computation** Considering the cold case scenario, the temperature of the spacecraft is the only unknown in the heat power balance and can therefore be calculated:

$$T_{sc} = \sqrt[4]{\frac{Q_{int} + Q_{IR,pl}}{\sigma (\epsilon_{sc} A_e + \epsilon_{rad} A_{rad})}} \quad (5.19)$$

where  $A_e = A - A_{rad}$ .

This temperature, 215,89 K, is too low, hence an heater sizing is necessary:

$$Q_{heaters} = \sigma (\epsilon_{sc} A_e + \epsilon_{rad} A_{rad}) T_{min}^4 - Q_{IR,pl} - Q_{int,min} \quad (5.20)$$

The power required by the heaters is around 18 kW.

### 5.2.5 Selected materials and subsystem budgets

As mentioned beforehand among the materials used for the external coating of the MetOp satellite is Aluminized Kapton. This material makes up a coat around the satellite body that is completely non-flammable in oxygen rich atmosphere. It can reflect up to 97 percent of sunlight and was appositely developed for in-space usage. As this is multi-Layered material both emissivity and absorptivity are tailored for space missions and are respectively 0.55 and 0.4. As the calculations show, however, this coating alone would not be enough and should be paired with the radiators. An optimal solution between thickness of the coating, surface of the radiators and mass should be searched iteratively. It shall also be considered that even though increasing the thickness of the coating does improve performance for the hot case, it makes it poorer for the cold one. As shown in the calculations listed above the total power needed to make the heaters work in order to provide optimal temperature windows for the

on-board instruments is 18 kW. This power is very high, this suggests different temperature management strategies are used for different parts of the spacecraft. This is why SVM and PLM use separate and differentiated system. Another strategy is to relax the temperature constraints of the instrumentation. This accounts for a less-capable TCS and therefore easier to size. Such solution is achieved putting the payload into a non-optimal temperature window. This has however effects on both the quality of the measurements and the life expectancy of the payload. Radiators' weight typically varies from almost nothing, if an existing structural panel is used as a radiator, to around 12 kg/m<sup>2</sup> for a heavy deployable radiator and its support structure. Assuming this last figure valid to design a worst-case scenario we obtain a total radiator's mass of 460.8 Kg. Such a high mass would affect significantly the mass budget and its location on the satellite would influence considerably its dynamics.

### 5.2.6 Subsystem layout

As previously discussed, the MetOp A satellite adopts different TCS layouts for the SVM and PLM due to different requirements in terms of power needed and function.



## Chapter 6

# Electric Power Generation and Storage Subsystem

Change Log	
6.1 System Architecture	Page 38: Section divided in "Solar Array", "Batteries" and "Power Regulation" subsections.
6.2 Reverse Sizing - Solar Array	Pages 39-40: "6.2.1 Power request" section revised; Added Table 6.1.
6.2.5 Surface and mass	Page 41: Values of solar array surface and mass revised.
6.2.6 Refined sizing	Page 42: Section revised.

The MetOp-A spacecraft needs to provide the necessary energy to operate its onboard systems, instruments, and communication devices throughout its mission. In order to accomplish those targets it is equipped with an electrical power system designed to provide the necessary power for its various systems and instruments throughout different phases of the mission, with different power budgets for every phase of the required task for the satellite.

The system is composed by solar arrays as a primary source of electrical power, and batteries as secondary and additional energy source. To complete the system there's a power distribution architecture that connects and delivers the correct amount of energy to the other subsystems during each phase of the mission.

MetOp-A is in a sun-synchronous orbit during the most of it's operative lifetime, meaning that it has to alternate the usage of solar arrays and batteries respectively during sunlight and eclipse phases. Also the batteries provide an additional amount of energy during the early operations of the mission and during orbital maneuvers.

Overall, the electrical power system of MetOp-A is designed to provide a reliable and continuous source of power to meet the mission's requirements, enabling the operation of various systems and instruments essential for meteorological and climate observations.

## 6.1 System Architecture

MetOp-A is powered by a large, eight-panel, solar array (SA), that works together with five 40 Ah batteries. SA provides electrical power to both Service Module and Payload Module for most of the time as when the satellite is not in eclipse, the ADCS subsystem targets SA directly towards the Sun. Batteries, instead, store the energy, allowing power supply during:

- Launch and Early Operations Phase (LEOP);

- time spent in eclipse;
- temporary power peak demand during sunlight.

### 6.1.1 Solar Array

Solar array consists of eight hinged solar panels, each 1 m x 5 m, equipped with BSR (back-surface reflector) solar cells, and it is able to generate a power of 3.890 kW at end-of-life. It is connected to the main body of the satellite through the primary deployment arm, a 4 m metallic tube, driven by Solar Array Drive Mechanism (SADM) mounted on the spacecraft side of the interface. It has two main functions: SA deployment during LEOP operations, and holding the correct orientation of solar array towards the Sun. Since the satellite is in a polar orbit, the Sun rises in the north when MetOp is passing over the south pole and settles in the south when passing over the north pole (it is at the equator at 21:30 local, the ascending node, and moving south). The Sun always shines from the left side, with a more or less constant angle of about 40° (with respect to the spacecraft body), therefore the solar array is mounted in order to have the Sun always at right angles to its surface, and it rotates around the east-west axis to compensate for the moving Sun. As already mentioned, the solar array was deployed during LEOP with a robotic arm of about 4m in length with three deployment hinges. The deployment arm accommodates around 300 power cables. In order to overcome the extremely cold conditions that could hinder the cables it was necessary to use not just thermal blankets but heaters to keep the cables warm. In addition, the cables were configured with large loops to form a compliant structure.

### 6.1.2 Batteries

For what concerns spacecraft's batteries, MetOp secondary power source, they are classified as secondary batteries because their technology allows to perform a high number of charge/discharge cycles. One of the most important parameters in this case is depth-of-discharge, DOD, that indicates the percentage of total battery capacity removed during a discharge period: for a satellite orbiting in LEO like this one, number of eclipses experienced during mission life is very high. As an example, if a satellite performs 15 charge/discharge cycles every day, this means a number of 5000 cycles per year, almost 40% of orbital period. MetOp batteries are reported to be the same as the Envisat spacecraft, which mounts Nickel Cadmium based batteries and can guarantee a 60% of DoD. Metop has on board five batteries that erogates 40 Ah of charge.

### 6.1.3 Power Regulation

The primary power bus is unregulated and distributes power to the service module and payload module units. The 28 V power regulation needed by the National Oceanic and Atmospheric Administration American instruments is provided by a dedicated Power Control Unit (PCU) located in the payload module. Power is controlled by a dedicated unit, named with the acronym RSJD, that is in charge of:

- balance among the power provided by the solar array;
- spacecraft power demand and batteries recharge;
- distribution of several power buses
- managing the batteries thermal control

- providing switch-off lines for the satellite management in case of failure conditions

The Power Distribution Unit (PDU) uses power from the Service Module to supply unregulated power (22–37.5 V) to all the payload module equipment and European instruments. To provide switching and protection functions, the PDU uses Latch Current Limiters, that provides over-current protection to payloads protecting the satellite power bus. The PDU also supplies power for the motor driven deployment of the Advanced Scatterometer instrument, Low Resolution Picture Transmission and Combined Receive Antenna (CRA) antennas.

## 6.2 Reverse Sizing - Solar Array

### 6.2.1 Power request

MetOp-A, being a meteorological satellite, operates in various modes during its mission to fulfill its different objectives and collect different types of data. Some of the common modes of operation for MetOp-A include:

- **Normal Mode:** In this mode, the satellite is in its standard operating configuration, continuously collecting data from its various instruments, such as the Advanced Scatterometer (ASCAT), the Advanced Very High-Resolution Radiometer (AVHRR), and the Global Ozone Monitoring Experiment (GOME). Normal mode is the primary operating mode for routine data acquisition.
- **Calibration Mode:** Periodically, the satellite may enter calibration mode to perform instrument calibrations and verify the accuracy of the collected data. Calibration is essential to ensure the data obtained is of high quality and accuracy.
- **Sun Observing Mode:** In this mode, the satellite is oriented to observe the Sun for calibration and monitoring purposes. This mode is particularly relevant for instruments that rely on solar observations.
- **Safe Mode:** If the satellite encounters any anomaly or potential threat to its operation, it may enter safe mode. Safe mode involves shutting down non-essential systems and pointing the satellite's solar panels directly at the Sun to ensure sufficient power supply.
- **Payload Modes:** Depending on the specific mission requirements and scientific objectives, the satellite may operate in different payload modes to focus on specific instruments or data collection tasks. For example, it may switch to a mode that prioritizes atmospheric observations or oceanic measurements.
- **Mission Planning Mode:** During this mode, the satellite is oriented and programmed to execute specific mission objectives, such as observing specific regions of the Earth's atmosphere or studying particular weather phenomena.

The power budget was analyzed considering the normal mode of the operational phase. Normal mode is the one in which the satellite gathers all of the scientific data from its sensors. The power budget analysis should also take into account the power demand of all the other subsystem that operates simultaneously. An approximate average power consumption of the different subsystem was estimated from the previous sizing and from the literature:

Subsystem	Average power demand
<b>Instruments</b>	898 W
ADCS	72 W
AMSU-A	99 W
ASCAT	215 W
AVHRR/3	27 W
GOME-2	42 W
GRAS	30 W
HIRS/4	24 W
IASI	210 W
MHS	93 W
S&RSAT	86 W
<b>TCS</b>	445 W
<b>AOCS</b>	180 W
<b>TTMTC</b>	140 W
<b>OBDH</b>	120 W
<b>Power</b>	50 W

Table 6.1: *Power demand*

Therefore the average power demand in the normal mode is approximately 1833 W. This result is in agreement with the MetOp-A effective consumption and with the typical power percentage distribution of a Metsat, which allocate 48% of total power (excluding the power destined to instrumentation) to thermal control, 19% to attitude control, 5% to power, 13% to command and data handling and 15% to communications. In order to take into account the possibility of power losses along the transmission lines and in order to guarantee a safety margin, it has been considered a higher value of power demand: 2 kW. Since the functioning of all the subsystems does not vary significantly from daylight mode to eclipse mode, the same average power demand was considered.

The first step is compute the power request to the SA with the following formula:

$$P_{SA} = \left( \frac{P_e T_e}{X_e T_d} + \frac{P_d}{X_d} \right) \quad (6.1)$$

where  $P_e$  is the power request in eclipse and  $P_d$  is the power request in daylight. Instead  $X_e$  and  $X_d$  are coefficients, respectively for eclipse and daylight, with two different values, depending on the power regulation technique used: one for the DET (Direct Energy Transfer) case and one for the PPT (Peak Power Tracking) case. In DET, the solar array is directly connected to the battery through a diode for protection; this technique requires a matching between the solar array and the batteries for having good efficiency. In PPT, power converters are used as interface between the solar array and the batteries for extracting the maximum power of the solar array; this requires more components and therefore PPT is more complex than DET. DET systems dissipates unneeded power: they typically use shunt resistors to maintain bus voltage at a predetermined level and shunt resistors are usually at the array or external banks of resistors to avoid internal heating. It is typical for systems less than 100 W. PPT extract the exact power required from the solar array: it uses DC to DC converter in series with the array, it dynamically changes the solar array's operating point and it requires 4-7% of the solar array power to operate. In view of the considerations above, it has been decided to analyze the case of a PPT regulation technique, which entails  $X_e = 0.6$  and  $X_d = 0.8$ .

$P_{SA}$  results roughly 3.77 kW.

### 6.2.2 Solar cells

MetOp-A's solar arrays mount triple-junction GaAs cells, they are chosen for their high power conversion with an efficiency ( $\epsilon_{BOL}$ ) about 30% and specific power product per unit mass ( $p$ ) of  $100 \frac{W}{m^2}$ . But they are sensible to aging, so it's detectable a degradation each year ( $dpy=0.0375$ ) and a inherent degradation factor ( $I_D=0.72$ ).

### 6.2.3 Power at BOL

The basic specific power output can be computed as:

$$P_0 = \epsilon_{BOL} I_0 \quad (6.2)$$

where  $I_0$  is the solar flux at a given distance. In our case  $I_0=1367.5 \left[\frac{W}{m^2}\right]$ .

So  $P_0=410.25 \left[\frac{W}{m^2}\right]$ .

At BOL we can also calculate the SA specific power produced with the formula:

$$P_{BOL} = P_0 I_D \cos \theta \quad (6.3)$$

with  $\theta$  as the average inclination angle between the array surface normal and the Sun direction that in the MetOp-A case is  $20^\circ$ .  $P_{BOL}=277,56 \left[\frac{W}{m^2}\right]$ .

### 6.2.4 Power at EOL

As mentioned before the solar cells tend to degrade in time, so in order to do a proper design we need to understand the specific power at the end of life. To achieve this result we first have to compute the lifetime degradation of the cells:

$$L_{life} = (1 - dpy)^{T_{life}} \quad (6.4)$$

In the beginning the mission was planned to end in 2015, so a  $T_{life}=9y$  that drive us to a  $L_{life}$  about 0.709. Therefore the SA specific power produced at EOL is:

$$P_{EOL} = L_{life} P_{BOL} \quad (6.5)$$

with a value of approximately  $196,8 \left[\frac{W}{m^2}\right]$ .

### 6.2.5 Surface and mass

To ensure the right production of power solar array's area have to be sized in this way:

$$A_{SA} = \frac{P_{SA}}{P_{EOL}} \quad (6.6)$$

that results approximately **19.17**  $[m^2]$ .

We can also calculate the solar cell mass knowing its relative surface density,  $\rho_{SA}=89 \text{ mg}/cm^2$ :

$$m_{SA} = \frac{A_{SA}}{\rho_{SA}} \quad (6.7)$$

for a value of **21.5 kg**, since Triple Junction Solar Cells InGaP/GaAs/Ge for Space Applications have a very low solar cell mass.

### 6.2.6 Refined sizing

In order to proceed into making a refined sizing for the solar array the following data is needed:

1. Single solar cell voltage  $V_{cell}$ , about 2.33 V
2. System voltage  $V_{sys}$ , up to 37.5 V
3. Single solar cell surface  $A_{cell}$ , about 30.15  $cm^2$

The first step that shall be done is computing the number of solar cells needed to cover up the entire SA surface according to the following formula:

$$N = \text{ceil}\left(\frac{A_{SA}}{A_{cell}}\right) \quad (6.8)$$

The number of total solar cells needed is **6358**.

In order to have more detailed informations about the layout of the solar cells we need to compute how many of them can be rearranged in a series.

$$N_{series} = \text{ceil}\left(\frac{V_{sys}}{V_{cell}}\right) \quad (6.9)$$

The number of cells per each series is: 17.

We can now obtain the real voltage as follows:

$$V_{real} = N_{series} V_{cell} \quad (6.10)$$

Real voltage is 39.61 [V]

The real number of cells is:

$$N_{real} = \text{ceil}\left(\frac{N}{N_{series}}\right) N_{series} \quad (6.11)$$

so, **since the total number of solar cells needed is exactly divisible for the number of cells per each series, the real number of cells is still 6358.**

Lastly, to end the SA sizing the real surface area is obtained as follows:

$$A_{SA,real} = N_{real} A_{cell} \quad (6.12)$$

Since  $N_{real}$  is equal to  $N$ , for the reason explained before, even the final area remains 19.17  $m^2$ . It is however important to notice that in this first evaluation of the dimensions of the solar array there is a strong approximation of the power demand, in particular of the TCS subsystem, since in first analysis it was not possible to determine the exact power consumption of the heaters. It is also relevant to say that the power demand used for this analysis is just the average: it doesn't take into account the peaks of power consumption. The safety margin imposed may be too low to cover the effects of these considerations. The final area computed is clearly underestimated with respect to the 40  $m^2$  used by EUMETSAT for the solar array of MetOp-A.

## 6.3 Reverse Sizing - Batteries

Batteries can be used as both a primary and secondary energy source, in our case we assume the SA to be our primary energy source, that is, if they can actually provide the system the power it needs, unlikely for eclipse phases.

There are architectural and material differences among primary and secondary batteries as they need to provide different power levels.

The following are the inputs for the battery sizing:

1.  $T_R$  [s] time in which batteries must provide power
2.  $P_R$  [W] Power required in the most critical mode
3.  $E_m$  [ $\frac{Wh}{kg}$ ] specific energy
4.  $E_v$  [ $\frac{Wh}{dm^3}$ ] energy density
5.  $\eta$  [-] line efficiency

The following formula can be used to compute the required capacity to fulfill power demand:

$$C = \frac{T_R P_R}{(DoD) N \eta} \quad (6.13)$$

N is the number of batteries and the MetOp-A satellite has five of them.

The capacity required is  $C = 313$  [Ah].

This calculation is performed assuming a time in which the batteries are needed of half equal to the longest possible eclipse time, that is, 28 minutes. Also, a worst case scenario power required of 1.81kW was considered. The mass needed for the batteries is:

$$m_{batt} = \frac{C}{E_m} \quad (6.14)$$

So 7.82 Kg are needed for our system.

The voltage of each individual battery is:

$$V_{batt} = \frac{C}{E_v} \quad (6.15)$$

Our batteries can provide a voltage of 3.47 V.

In order to obtain a refined sizing of the batteries, the single battery cell voltage and the system voltage are needed. From literature we could find that Ni-Cd cells have a nominal voltage of 1.2 V. The regulated power lines for SVM/PLM units have 50 V

$$N_{series} = ceil(\frac{V_{sys}}{V_{cell}}) \quad (6.16)$$

The actual number of series is then 42.

$$V_{real} = N_{series} V_{cell} \quad (6.17)$$

Therefore, the real voltage is 50.4V.

The capacity of the single string is:

$$C_{string} = \mu C_{cell} V_{real} \quad (6.18)$$

Giving us 20.16 Ah.

The actual number of strings is:

$$N_{parallel} = ceil(\frac{C}{C_{string}}) \quad (6.19)$$

Giving us a total of 16 parallel strings.

Lastly, the actual battery system capacity is

$$C_{real} = N_{parallel} C_{string} \quad (6.20)$$

Giving us a real capacity of 322.6 Ah.

## Chapter 7

# Configuration of Space Segment

In the following chapter a brief overview about the MetOp-A satellite's configuration will be discussed. With "configuration" we mean the study of the location of all the components on board, made in such way that the most equipment as possible works at its best and that as little adjustments as possible are needed throughout the mission. The configuration of the spacecraft is influenced by a number of factors and they will be analyzed later on. One of the simplest, yet crucial, aspect that heavily influences the configuration is the geometry of the satellite. Geometry-based requirements are of two kinds (primarily):

- Dynamic-related
- Size related

An example of a dynamic-related requirement could be arranging the on-board systems in such way that the excursion of the satellite's CG is kept confined within a given value. To meet such requirements, for instance, a solution could be placing tanks strategically. A size related requirement could, for instance, be the compatibility with the launcher in order to accommodate the craft in the fairing bay. This requires the study of the configuration for both the packed and unpacked configurations. For instance, the MetOp-A satellite was launched using the Soyuz/ST launcher using the ST (81KS) fairings, meaning a 4.11 meter fairing was available. Among other configuration drivers are:

- Instruments FOV: an instrument whose FOV is hampered damages the outcome of the mission.
- Heat Rejection: elements of the TCS can't be facing the Sun constantly.
- Inertia: Effects the dynamics of the satellite.

## 7.1 MetOP-A's CONF

As mentioned before once the launcher is selected some geometric layouts are imposed by the internal volume of the cargo bay. In order to make the MetOp-A satellite compliant with the cargo volume available in the ST(81KS) fairings the body of the satellite was designed as a parallelepiped-shaped box with its X axis along its greater dimension.

Figure 7.2 also shows how the thrusters for the attitude control are strategically located to generate torque around all three axis as well as propulsion over the +Y/-Y axis. Tanks are located towards the center of the satellite to reduce the CG drift as much as possible. To do so their longer dimension is aligned with the X axis. Tanks are 4 and radially mounted with a 90 degree angle phase along the before mentioned axis. In order to free up as much space



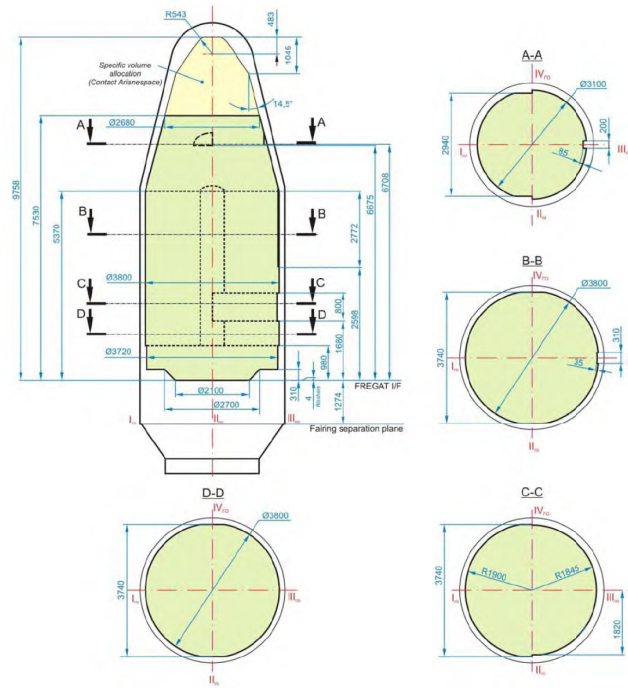


Figure 7.1: Fairing dimensions

as possible on the surface, the solar panel array is actually detached from the spacecraft. As a foldable design was chosen this did not affect the packed configuration. This design choice is unusual, as symmetrical configurations make it easier to control the CG drift, at least along one axis; this configuration, however, maximizes both the available space for the instruments along the core of the satellite and their FOV. The batteries are mounted where the solar array mount is connected to the body of the satellite to reduce the amount of wiring needed and allow the batteries to operate all at the same temperature, granting close to identical performance among them. It's important to notice that the +X face is empty as it is aligned with the velocity vector. This solution allows to protect the on board payload from all the charged particles trapped at that altitude by the interaction of the inner and outer magnetic fields. The payload is stored on board mainly on the -Y face which is the one always facing the Earth. In order to increase the FOV of each instruments ASCAT antennas do stick out of the body, and in order to maximize their capability of collecting data are conveniently offsetted. +Y face is essentially free and used for thermal dissipation purposes. Antennas face down the earth in order to require as little attitude corrections as possible to grant optimal orientation. It must be notice that a structural and dynamical analysis would be required to find the best configuration for all the components, however, this is not the goal of this paper. The payload distribution is shown in Figure 7.3 where instead Figure 7.4 shows the entire spacecraft with also service module.

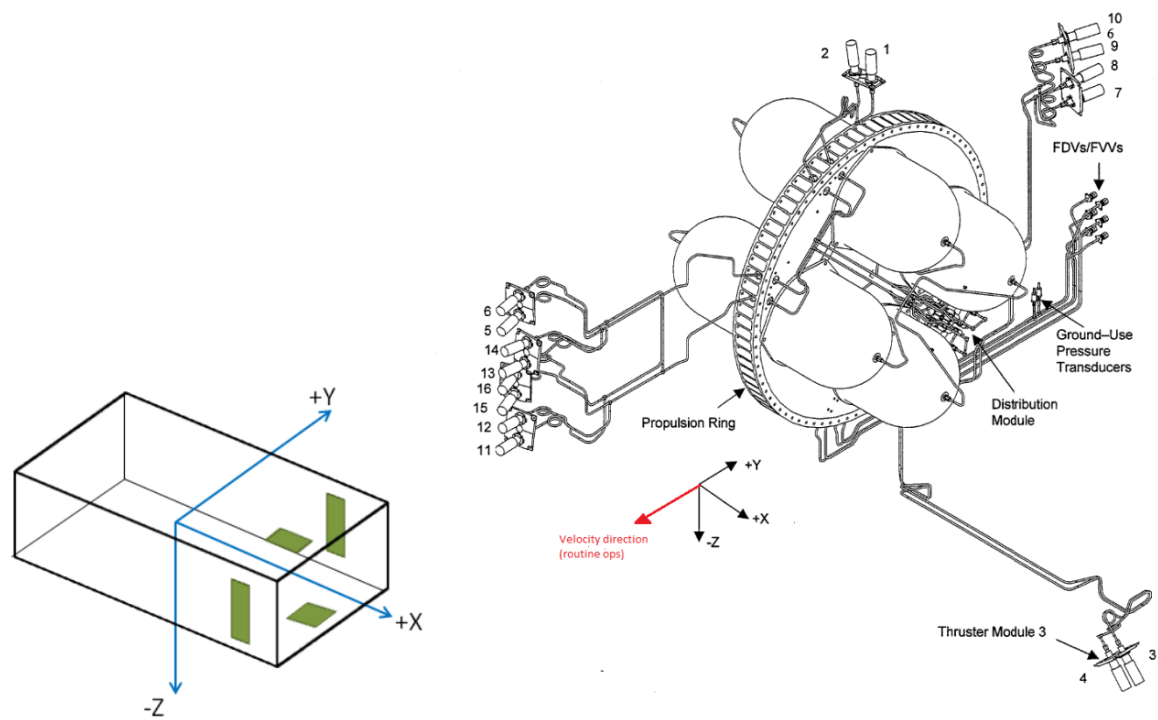


Figure 7.2: MetOp-A engines disposition



Figure 7.3: MetOp-A payload distribution

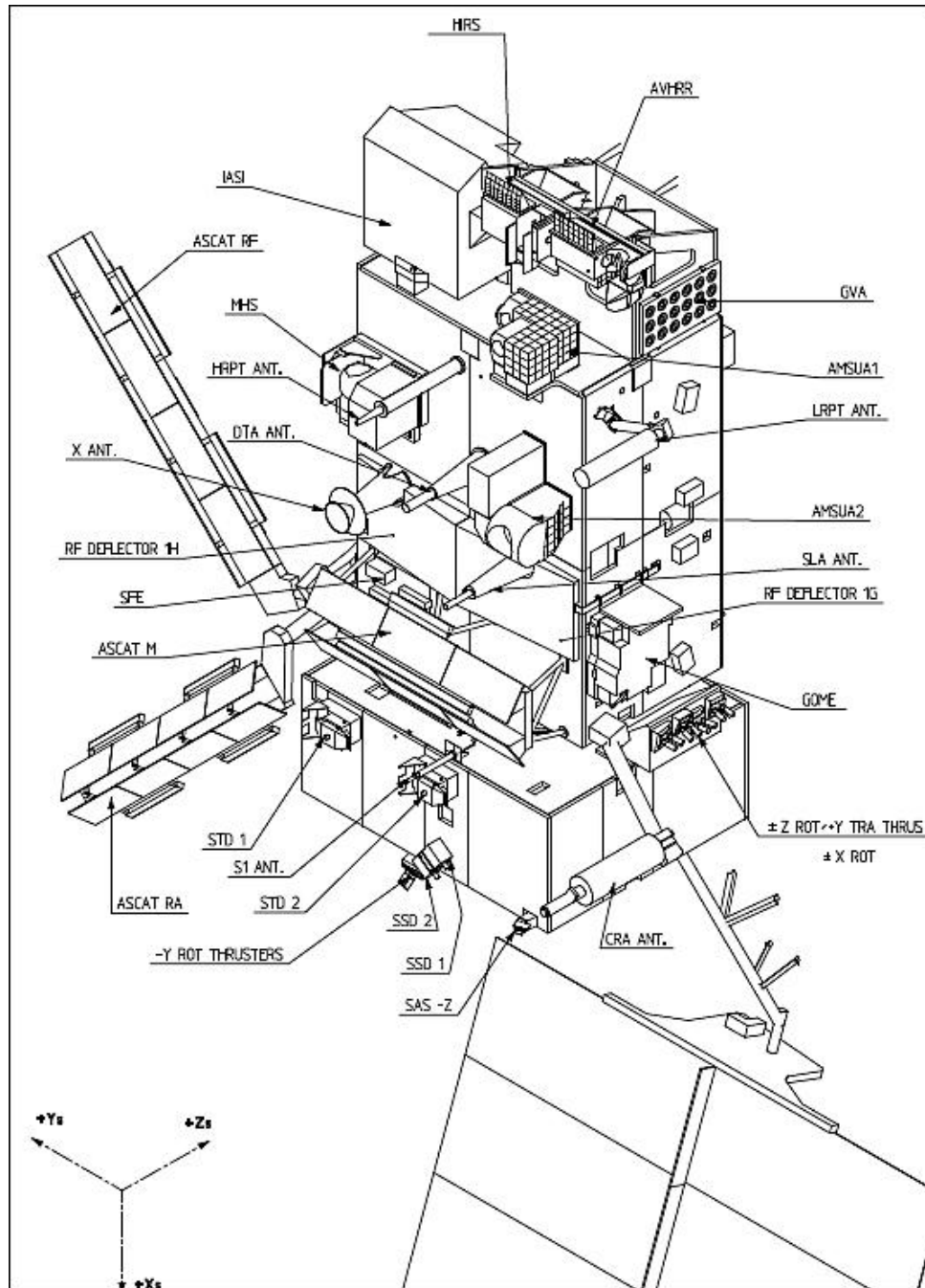


Figure 7.4: Line drawing of the MetOp-A spacecraft

## Chapter 8

# On-Board Data Handling Subsystem

The on-board data handling system of a spacecraft like MetOp-A is responsible for managing and processing the vast amount of data collected by its instruments and subsystems. It plays a crucial role in storing, transmitting, and analyzing data to fulfill the mission objectives. The data handling system collects data from various instruments and sensors on board the spacecraft. This can include measurements of atmospheric parameters, sea surface temperature, land surface conditions, and other relevant environmental data. The collected data are often compressed to reduce their size for efficient storage and transmission by employing algorithms and techniques to compress data while preserving their essential information. The on-board data handling system performs certain data processing tasks to extract valuable information from the collected data. This can include applying calibration algorithms, removing noise, enhancing image quality, or deriving parameters from raw measurements. Data processing is often done in real-time or near-real-time to support mission operations and decision-making. The data handling system is responsible for transmitting selected data to ground stations or other receiving systems. It coordinates the data down-link process, including scheduling, prioritization, and error checking to ensure reliable transmission. The specific design and capabilities of the on-board data handling system for MetOp-A are tailored to the mission's requirements, including the types and volume of data collected, real-time processing needs, and the down-link capabilities of the spacecraft.

### 8.1 System Architecture

Data handling architecture of MetOp-A is decentralised, the Payload Module and Service Module have their own computer. Primary spacecraft computer is on SVM and it is a MA 31750 microprocessor with two redundant memory modules of 224 kwords, called Central Communication Unit, CCU. It is responsible for the interface to the ground segment, for the control of the equipment and for the overall security of the mission. Command and control of the Payload Module is performed by PLM Computer, PMC, connected to CCU via SVM OBDH bus. PMC receives instructions from SVM computer and interfaces with:

- European instruments ICUs, Instruments Control Units;
- MPU, MHS PLM adaptation Unit;
- NIU, NOAA Interface Unit, a specific unit for US instruments.

MHS is the only payload instrument with an adaption unit with PMC because it is the only one based on the MIL-STD-1553 interface, an high-level command and control interface just like European OBDH one. NIU performs command and control through a dedicated ICU and

collects measurement data, processed by a Digital Signal Processor omtp CCSDS packets. It also performs AVHRR data compression.

Science data from payload is provided at a wide range of data rates, from 1.5 Mbps for IASI, to 160 bps for SEM. PMC also provides some additional packets required for data exploitation, such as position and time data derived from GRAS, or a copy of the full spacecraft housekeeping telemetry. All of these data streams are multiplexed and provided on three channels going to onboard recorder, HRPT and LRPT direct-broadcast subsystems.

Global coverage of measurement data is achieved by a recording of all data over a complete orbit on Solid State Recorder, SSR, based on Cluster and Envisat design. It has a capacity of 70 GB EOL, sufficient to provide the necessary internal redundancies as well as to cover worst-case down-link. Simultaneous recording and dumping is supported such that special measures to avoid data losses during down-link are not required: during ground station pass, also the measurement data acquired during the pass can be immediately down-linked together with dumping of the recorder.

## 8.2 Reverse Sizing

### 8.2.1 OBC features

In order to determine preliminary the memory and the performance needed from the on-board computer it is used the "Estimation by similarity" approach. This method is used to retrieve average data from statistics, in particular it allows to estimate the codes and memory data for each function allocated to the computer, along with throughput requirements and typical frequencies. The first step is then to identify, for each subsystem, all the functions that the computer has to handle and their average features.

With these data, and imposing also the acquisition frequency of the computer, it is possible to compute by-similarity the throughput needed by each function:

$$KIPS = \frac{KIPS_{typ} f}{f_{typ}} \quad (8.1)$$

The results are:

ADCS							
Components	N°	Code	Data	Typical KIPS	Typical Frequency	Acquisition Frequency	Final KIPS
Reaction Wheels Control	3	1000,0	300,0	5,0	2,0	1,0	2,5
Thruster Control	16	600,0	400,0	1,2	2,0	1,0	0,6
Magnetic Control	2	1000,0	200,0	1,0	2,0	1,0	0,5
IMU	4	800,0	500,0	9,0	10,0	10,0	9,0
Sun Sensors	2	500,0	100,0	1,0	1,0	1,0	1,0
Earth Sensors	2	1500,0	800,0	12,0	10,0	10,0	12,0
Kinematic Integration	1	2000,0	200,0	15,0	10,0	10,0	15,0
Error determination	1	1000,0	100,0	12,0	10,0	10,0	12,0
Attitude determination	1	15000,0	3500,0	150,0	10,0	10,0	150,0
Attitude control	1	24000,0	4200,0	60,0	10,0	10,0	60,0
Complex Ephemerides	1	3500,0	2500,0	4,0	0,5	1,0	8,0
Orbit Propagation	1	13000,0	4000,0	20,0	1,0	1,0	20,0

Table 8.1: *OBDH functions of ADCS*

PS							
Components	N°	Code	Data	Typical KIPS	Typical Frequency	Acquisition Frequency	Final KIPS
Main Engine	8	1200,0	1500,0	5,0	0,1	0,1	5,0
Tank Control Valve	10	800,0	1500,0	3,0	0,1	0,1	3,0
Tank Pressure Sensor	4	800,0	1500,0	3,0	0,1	0,1	3,0

Table 8.2: *OBDH functions for PS*

EPS							
Components	N°	Code	Data	Typical KIPS	Typical Frequency	Acquisition Frequency	Final KIPS
Power Voltage Control	1	1200,0	500,0	5,0	1,0	0,1	0,5
Power Current Control	1	1200,0	500,0	5,0	1,0	0,1	0,5

Table 8.3: *OBDH functions for EPS*

TCS							
Components	N°	Code	Data	Typical KIPS	Typical Frequency	Acquisition Frequency	Final KIPS
Thermal Control	2	800,0	1500,0	3,0	0,1	0,1	3,0

Table 8.4: *OBDH functions for TCS*

TT&C							
Components	N°	Code	Data	Typical KIPS	Typical Frequency	Acquisition Frequency	Final KIPS
Transponder Up-link	2	1000,0	4000,0	7,0	10,0	10,0	7,0
Transponder Down-link	6	1000,0	2500,0	3,0	10,0	10,0	3,0

Table 8.5: *OBDH functions for TTMTTC subsystem*

OS							
Components	N°	Code	Data	Typical KIPS	Typical Frequency	Acquisition Frequency	Final KIPS
I/O Device Handlers	1	2000,0	700,0	50,0	5,0	1,0	10,0
Test and Diagnostic	1	700,0	400,0	0,5	0,1	1,0	5,0
Math Utilities	1	1200,0	200,0	0,5	0,1	1,0	5,0
Executive	1	3500,0	2000,0	60,0	10,0	10,0	60,0
Run Time Kernel	1	8000,0	4000,0	60,0	10,0	10,0	60,0
Complex Autonomy	1	15000,0	10000,0	20,0	10,0	10,0	20,0
Fault Detection	1	4000,0	1000,0	15,0	5,0	1,0	3,0
Fault Correction	1	2000,0	10000,0	5,0	5,0	10,0	10,0

Table 8.6: *OBDH functions for satellite's operative system*

A higher acquisition frequency is required from those function that needs to process rapidly important data for the control of the satellite; a lower frequency can be used for less vital functions.

After these first steps it is possible to calculate the total throughput, as well as the total data and the total codes, needed by each subsystem while in different modes of the mission. This can be done with a simple sum of the codes, data and throughput of each single function.

$$KIPS_{TOT} = \sum k_{fun} KIPS_{fun} \quad (8.2)$$

$$Data_{TOT} = \sum k_{fun} Data_{fun} \quad (8.3)$$

$$Code_{TOT} = \sum k_{fun} Code_{fun} \quad (8.4)$$

The different modes in which MetOp-A works are communication and maneuvering, other than scientific mode which is not considered in this preliminary analysis since the instruments data are processed separately by the PLM computer.

Communication	ADCS	PS	EPS	TCS	TT&C	OS	TOT	Margined
Throughput	343.5	0	1	6	32	173	555.5	2777.5
Code	80300	0	2400	1600	8000	36400	128700	643500
Data	26000	0	1000	3000	23000	28300	81300	406500
Manoeuvring	ADCS	PS	EPS	TCS	TT&C	OS	TOT	Margined
Throughput	343.5	82	1	6	0	173	605.5	3027.5
Code	80300	20800	2400	1600	0	36400	141500	707500
Data	26000	33000	1000	3000	0	28300	91300	456500

Table 8.7: *Total throughput needed by each subsystem during different modes*

It is important to consider a high margin, typically around 400%, since it is a very preliminary analysis based on statistical data and it's therefore mandatory to be as much conservative as possible in order to not underestimate the size of the subsystem.

### 8.2.2 On-board memory size

Having determined all the OBC features it is possible to perform the memory sizing.

**ROM: Read-Only Memory** It stores data that are permanent and therefore that can be read but not altered. ROMS are also nonvolatile: when electrical power is removed from the devices they do not lose the data that are stored in them. Typical s/c computers have from 1 MB to 64 MB (8-bit words).

It can be computed as:

$$ROM[kb] = \frac{Code[word] 16[\frac{bit}{word}]}{8[\frac{bit}{byte}] 1000[\frac{byte}{kbyte}]} \quad (8.5)$$

The required ROM result to be 1287 kbyte for the Communication mode and 1415 kbyte for the Manoeuvring mode.

**RAM: Random Access Memory** It stores non-permanent data, which are volatile: if power to the devices is interrupted then the data stored in memory are lost. RAM is often the fastest kind of memory and it allows data items to be read or written in almost the same amount of time irrespective of the physical location of data inside the memory. Typical

s/c computers have from 4 MB to 256 MB of RAM.

It can be computed using the formula:

$$RAM[kb] = \frac{(Code[words] + Data[words])16[\frac{bit}{word}]}{8[\frac{bit}{byte}]1000[\frac{byte}{kbyte}]} \quad (8.6)$$

The required RAM result to be 2100 kbyte for the first mode and 2328 kbyte for the second one.

**TP: Throughput** The required performance for the on-board computer is determined by the total throughput, measured in MIPS. It's therefore necessary a simple conversion of the previously computed total throughput from KIPS to MIPS.

$$TP[MIPS] = \frac{KIPS_{TOT}[KIPS]}{1000[\frac{KIPS}{MIPS}]} \quad (8.7)$$

The result is approximately 2.8 MIPS for the Communication mode and 3 MIPS for the Manoeuvring mode.

In all three cases the most stringent requirements are given by the Manoeuvring mode; therefore the OBDH budgets, considering a 400% margin, are: ROM>1.415 Mb, RAM>2.328 Mb and TP=3 MIPS.

As already mentioned, since this constitute a preliminary analysis, it has been imposed a high margin. However, it is possible to gradually refine the estimates with the progress of the design. The non-margined budgets, in fact, are roughly 0.6 MIPS and 0.4 Mbyte, which fall within the capabilities of the MA31750 microprocessor selected by EUMESTAT.



# Bibliography

- [1] Antimo Damiano, Pier Luigi Righetti, Anders Soerensen. *Operational Local Time And Eccentricity Management for METOP-A*. RHEA Systems S.A. at EUMETSAT, Eumetsat Allee 1, D-64295 Darmstadt, Germany
- [2] Y. Buhler, M. Cohen, M. Rattenborg, M. Williams, P. Ranzoli. *The EUMETSAT Polar System: From Launch Preparation to Entry into Operations*. EUMETSAT, Am Kavalleriesand 31, D-64295 Darmstadt, Germany
- [3] Marco Buemi, Jean-Michel Caujolle, Luis Huertas Martin. *Metop-A Satellite In Orbit Verification: the challenge*. EUMETSAT, Am Kavalleriesand 31 , 64295 Darmstadt, Germany
- [4] Yves Buhler, Jean-Michel Caujolle. *Preparing MetOp for Work: Launch, Early Operations and Commissioning*. Eumetsat, Darmstadt, Germany
- [5] Pier Luigi Righetti, Hilda Meixner, Francisco Sancho, Antimo Damiano, David Lazaro. *Flight Dynamics Performances Of The Metop-A Satellite During The First Months Of Operations*. Am Kavalleriesand 31, Darmstadt, D-64295, Germany
- [6] Pierluigi Righetti, Jose Maria de Juana Gamo and Richard Dyer. *Mission Analysis of MetOp-A End-Of-Life Operations*. EUMETSAT Allee, D-64295 Darmstadt.
- [7] Pier Luigi Righetti, Richard Dyer. *Feasibility of MetOp-A Mission Extension on Drifting Local Time*. EUMETSAT, Darmstadt, Germany
- [8] P.G. Edwards, D. Pawlak, *Metop: The Space Segment for Eumetsat's Polar System*
- [9] J. E. Fernhdez del Rio, A. Nubla, L. Bustamante, K. van't Klooster, *SOPERA: A New Antenna Concept for Low Earth Orbit Satellites*
- [10] V. Galindo, K. Green, *A Near-Isotropic Circularly Polarized Antenna for Space Vehicles*
- [11] R. Skatteboe, A.A.Kjeldsen, *Interoperability reduces cost and risk at Svalbard Satellite Station*
- [12] F. Sancho, D. Lazaro, P. Righetti. *Out-of-plane manoeuvre campaigns for MetOp-A: planning, modelling, calibration and reconstruction*.
- [13] C. Crozat, P. Righetti, L. De La Taille, F. Perlik, P. Collins. *MetOp-A Attitude and Orbit Control Operations*. SpaceOps 2008 conference, ESA and EUMETSAT iin association with AIAA, 2008.
- [14] Y. T. Noon, P. Righetti. *Precise calibration of multi-segment manoeuvres for EUMETSAT Polar System (EPS) operations planning*.
- [15] NASA Space Vehicle Design Criteria. Spacecraft Magnetic Torque
- [16] NASA Space Vehicle Design Criteria. Spacecraft Radiation Torque

- [17] MetOp-A Eoportat section
- [18] Bradford Space Reaction Wheel Unit datasheet
- [19] Pipoli T., Hendel B., Dudley G., Schautz M. *Evaluation of Maximum Safe Voltage for Nickel-Cadmium Cells*
- [20] Sanat Pandey. *Ge/GaAs/InGaP Triple-Junction Solar Cells for Space Exploration*. Department of Electrical and Computer Engineering, University of Illinois, Illinois, USA
- [21] CESI S.p.A., *Triple-Junction Solar Cell for Space Applications (CTJ30)*
- [22] Claudinei J. Donato, Cairo L. Nascimento Jr., Geraldo J. Adabo, *Design and Implementation of a Power Control Unit for the Solar Array of the ITASAT University Satellite*
- [23] Jesus Gonzalez-Llorente, Eduardo Ortiz-Rivera. *Comparison of Maximum Power Point Techniques in Electrical Power Systems of CubeSats*
- [24] David W. Miller, John Keesee. *Spacecraft Power Systems*